R-08-131

Backfilling and closure of the deep repository

Phase 3 – pilot tests to verify engineering feasibility

Geotechnical investigations made on unsaturated backfill materials

Lars-Erik Johannesson, Clay Technology AB

December 2008

Svensk Kärnbränslehantering AB
Swedish Nuclear Fuel
and Waste Management Co

Box 250, SE-101 24 Stockholm
Phone +46 8 459 84 00

ISSN 1402-3091
SKB Rapport R-08-131

Backfilling and closure of the deep repository

Phase 3 – pilot tests to verify engineering feasibility

Geotechnical investigations made on unsaturated backfill materials

Lars-Erik Johannesson, Clay Technology AB

December 2008

Contents

1 Introduction

The investigations described in this report is a part of the third phase of the joint SKB-Posiva project "*Backfilling and Closure of the Deep Repository, BACLO*". The overall objective of the BACLO project is to develop backfilling concept for the deep repository that can be configured to meet SKB's and Posiva's requirements in the chosen repository sites /1-1/. The project was divided into four phases, of which two have already been performed. The second phase of the BACLO project consisted of laboratory tests and deepened analyses of the investigated backfill materials and methods and resulted in recommendation to focus on the development and testing of the block placement concept with three alternative backfill materials /1-2/. The third phase investigations comprise of laboratory and large-scale experiments aiming at testing the engineering feasibility of the concept. In addition, how site-specific constraints, backfilling method & materials affect the long-term functions of the barriers will be described and analysed in order to set design specifications for the backfill.

The third phase of the BACLO project is divided into several subprojects. The work described in this report belongs to subproject 1 concerning *processes during installation and saturation* of the backfill that may affect the long-term function of the bentonite buffer and the backfill itself.

One of the main functions of backfill is to restrict buffer expansion which can lead to decrease in buffer density in the deposition hole. The criterion used as a basis for the Baclo investigations was that the buffer density at saturation should not be below 1,950 kg/m^3 at the level of the canister /1-1/. The same criterion was applied for the work described in this report. The upward swelling of the buffer and the enclosed compression of the backfill was first studied assuming that both the buffer and the backfill were saturated /1-3/. The main objective of this work was to study a case where the buffer is fully saturated while the backfill consisting of pre-compacted blocks and pellet filling are assumed to be unsaturated. This scenario was chosen because it was estimated that in reality the situation would be somewhere between these two cases. Calculations of the swelling of the buffer and deformation of the backfill were made with different types of backfill materials. The compressibility of the pellet filling and the compacted blocks were studied with laboratory measurements to produce input data for the calculations. Furthermore, the strength of the compacted backfill materials was investigated as well as hydraulic conductivity and swelling pressure for the investigated backfill materials in densities expected in block backfill.

2 Materials used in the tests

2.1 General

The tests described in this report are made with following materials:

- Indian bentonite (produced by Ashapura) named **Asha 230 bentonite**.
- German mixed-layer expandable clay named **Friedland clay**.
- **30/70 mixture** consisting of IBECO Deponit CAN Ca-bentonite (30%) and crushed rock (70%).

The samples were prepared with distilled water. Saline water (3.5% and 7%, NaCl:$CaCl_2$ 50:50) was used when investigating the hydraulic conductivity and swelling pressure.

Measurements of the compressibility of different type of pellets were also performed. The tests were made with the following type of pellets and granules:

- **Cebogel QSE** is a commercial bentonite pellet product with a montmorillonite content of about 80%. The pellets were delivered by Cebo Holland BV. The pellets are extruded cylindrical rods with a diameter of 6.5 mm and a length of 5–20 mm.
- **Minelco granules** consist of Na-activated Ca-bentonite from Milos, Greece. The granule size distribution of material is very inhomogeneous (55% is > than 4 mm and 99% > 1 mm).
- **Friedland granules** consist of mixed layer clay from Germany with a smectite content of about 45%. The material consists of broken fragments. The pieces are even-grained with a size of about 8 × 8 × 4 mm.
- **MX-80** pellets that were especially made for SKB consist of MX-80 Wyoming bentonite with a smectite content of about 75–80%. The pellets are pillow shaped with the dimensions 18 × 18 × 8 mm. In addition there are a few percent fine material.

2.2 Classification

"Geotechnical index tests" for Asha 230 and Friedland clay have been done in Phase 2 of this project. The tests included compaction tests, hydraulic conductivity and swelling pressure tests (at three different densities and with a water salinity of 3.5%), normalised free swelling test and determination of the liquid limit. The tests are described in /1-3/.

A new batch of the two clays Asha 230 and Friedland has been used in this part of the project. Additional "Geotechnical index tests" have been performed on the new batches. The results from the tests are summarised in Table 2-1 together with the previous tests. The parameters for MX-80 are also included in the table as a reference.

The initial water content, defined as the weight of the water in the sample divided with the weight of the solid particles, varied between 0.7 and 17%. The lowest water ratio was measured on Asha 230 B which was dried and crushed before it was used for the tests.

For determination of the normalized free swelling, 1.1 g clay (corresponding to 1.0 g of dry clay) was carefully poured in a measuring glass filled with 100 ml de-ionized water. The water content of the material was also determined. After 24 hours the volume of the clay gel was determined and normalized with respect to the weight of solid particles. The measured value for MX-80 is about 15–20 ml. The free swelling volume of the other clays is significant lower than for the Wyoming bentonite (see Table 2-1).

The definition of the liquid limit (w_L) of a soil is the water content where the soil transforms from plastic to liquid state. This parameter is for a bentonite correlated to parameters as swelling pressure and hydraulic conductivity. The liquid limit was determined with the fall-cone method. The method is described by the Swedish Geotechnical Society (SGF) /2-1/. Due to the thixotropic behavior of bentonite the fall cone tests is made 24 h after the preparation of the specimen (which is an aberration form the standard). The measured liquid limit for MX-80 is 450–550%. The liquid limit for the rest of the clays is significantly lower except for Asha 230B implying that the smectite content of the second delivery of Asha bentonite is significantly higher than of the first one (Table 2-1).

The ballast used for the 30/70 mixture is called Ballast B and it was delivered by Posiva and is further described in /2-2/. The grain size distribution of the ballast material is shown in Figure 2-1.

Table 2-1. Characterisation of the used clays.

Clay type	Initial water ratio (%)	Normalised free swelling (ml)	Liquid limit (%)
Asha 230	15.6	8.4	180
Asha 230 B	0.7	13.5	473
Friedland	6.4	7.7	109
Friedland B	8.4	4.3	112
Deponit CA-N	16.3	5.3	157
MX-80	8.8	20.8	524

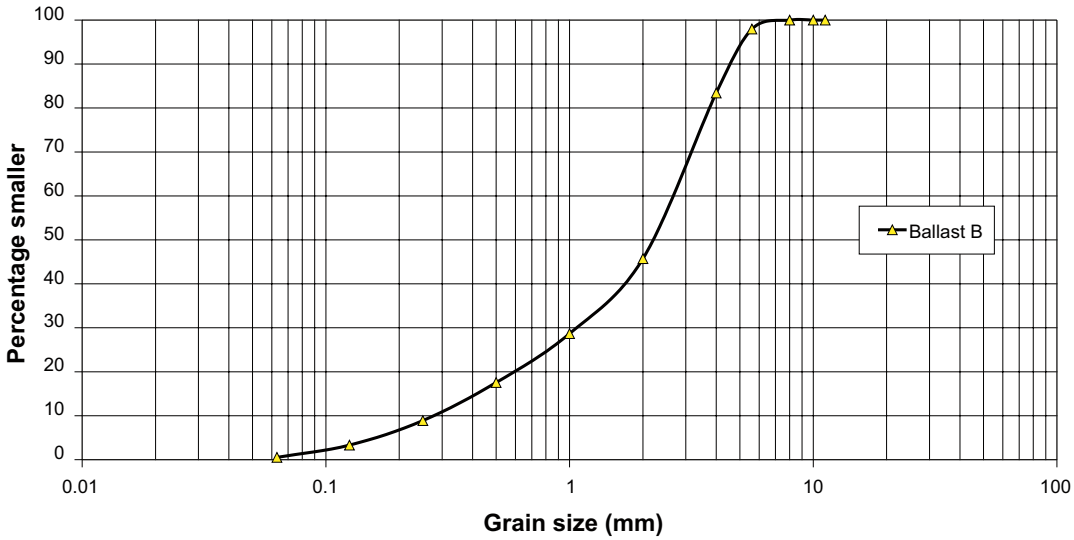

Figure 2-1. *Grain size distribution of the ballast material.*

3 Evaluation of elastic parameters of unsaturated backfill

To be able to evaluate the compression of unsaturated backfill material at a stage when the buffer is saturated and a swelling pressure from the buffer is acting on the backfill, the elastic parameters Young's modulus and the Poisson ratio of the backfill blocks are required. The tests to evaluate the parameters were made as follows:

- Small samples were made with uniaxial compaction in a mould with rigid walls with a compaction pressure of about 25 MPa (Ø 35 mm, h 60 mm). The water ratio of the different materials were chosen according to earlier compaction tests /1-3/ in order to get the maximum dry density.
- The samples were placed in a load frame and compressed in axial direction without lateral support. The deformation of the samples (vertical and horizontal) together with the applied load (see Figure 3-1) were measured during the test.
- The evaluation of Young's modulus (E) and Poisson ratio (ν) were made with the following equations:

$$E = \frac{\Delta\sigma_v}{\Delta\varepsilon_v} = \frac{\Delta P \times L}{A \times \Delta L} \tag{3-1}$$

$$\nu = -\frac{\varepsilon_h}{\varepsilon_v} = \frac{\Delta W \times L}{W \times \Delta L} \tag{3-2}$$

where
$\Delta\sigma_v$ = Vertical stress (kPa)
$\Delta\varepsilon_v$ = Vertical strain
ΔP = Applied load (kN)
L = Sample length (m)
ΔL = Change in sample length (m)
A = Area of the sample (m^2)
ε_v = Vertical strain of the sample
ε_h = Horizontal strain of the sample
W = Sample diameter
ΔW = Change in sample diameter (m)

Typical results from the measurements are shown in Figure 3-2. Young's modulus was determined from a straight line applied to the test data. The interpretation of the modulus was made in the stress interval between 0–2,500 kPa. Poisson ratio was determined from the measurements made of the horizontal strain of the samples, see Figure 3-2. The horizontal strain was measured in two perpendicular directions of the sample and the average the measurement was used for the interpretation. The measurements for all the performed tests are presented in Appendix 1 and the interpreted parameters are summarized in Table 3-1.

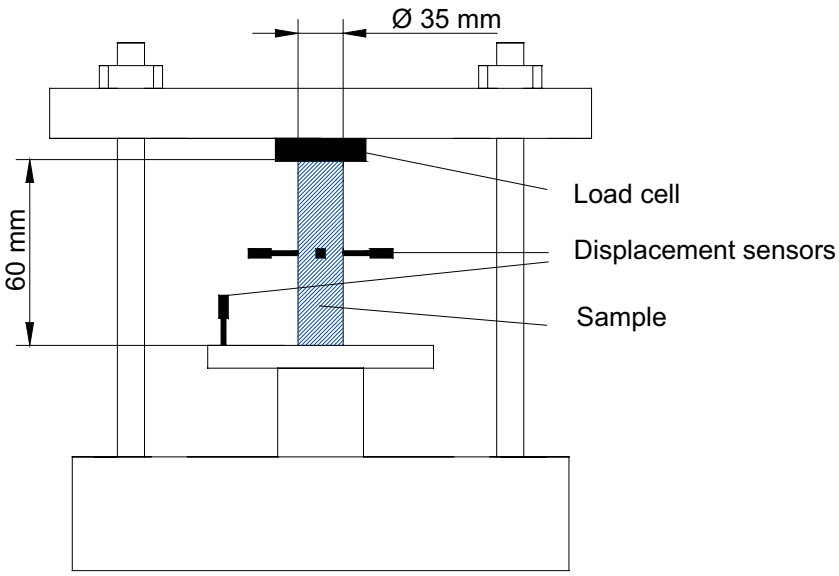

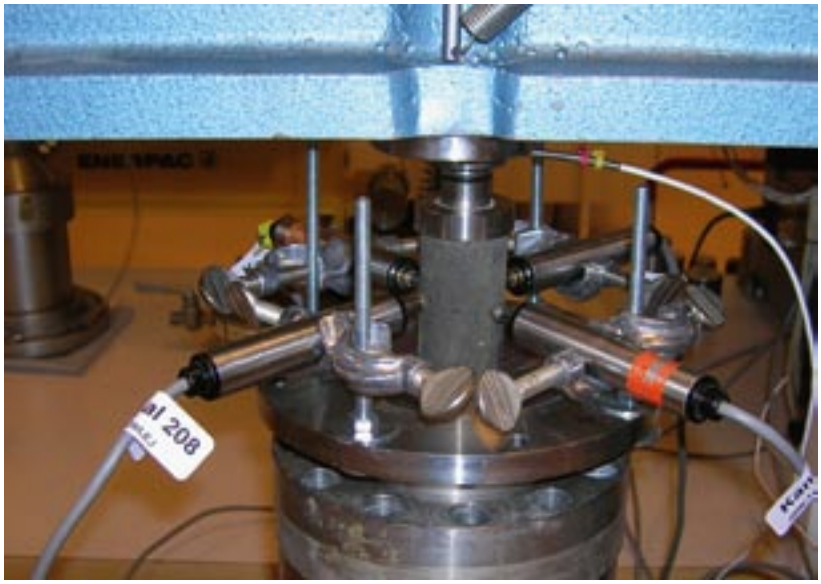

Figure 3-1. *Test arrangement for determination of the Young's modulus and the Poisson ratio on pre-compacted backfill materials.*

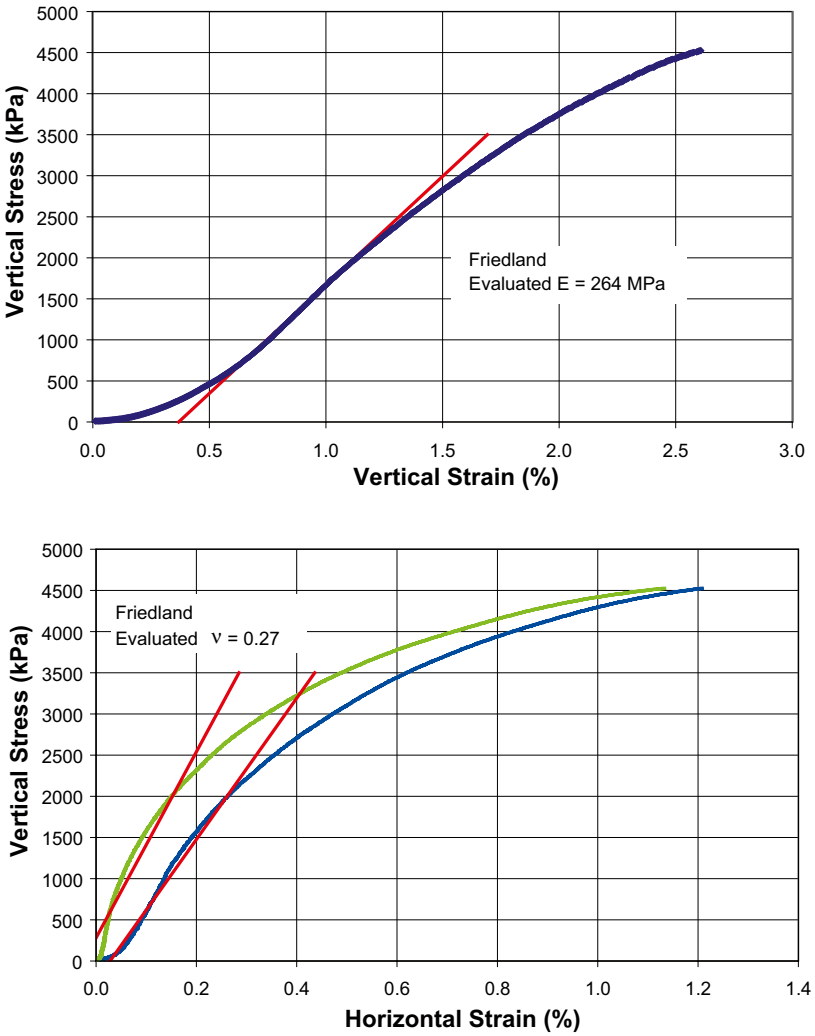

Figure 3-2. Measurements of the vertical strain and the horizontal strain in two directions used for determining the Young's modulus and Poisson ratio on Friedland clay.

Table 3-1. Evaluated Young's modulus and Poisson ratio for the investigated backfill materials.

Test No	Mtrl	Dry density (kg/m³)	Water ratio	E-modulus (MPa)	*v*
2	Friedland	2,047	0.094	264	0.27
3	Friedland	2,058	0.091	297	0.22
4	Friedland	2,064	0.089	256	0.24
5	30/70 mix	2,175	0.060	177	0.24
6	30/70 mix	2,173	0.059	212	0.19
7	30/70 mix	2,171	0.063	265	0.11
8	Asha 230 B	1,679	0.171	244	0.11
9	Asha 230 B	1,692	0.168	265	0.13
10	Asha 230 B	1,693	0.174	250	0.09
11	Asha 230 B	1,684	0.172	244	0.08
12	Asha 230 B	1,689	0.172	248	0.09
13	Asha 230 B	1,698	0.173	256	0.09

4 Evaluation of the strength of blocks of backfill materials

The strength of the pre-compacted blocks of backfill material was determined with two different test types:

1. Unconfined one dimensional compression tests
2. Beam tests

4.1 Unconfined one dimensional compression tests

For the unconfined one dimensional compression tests, the samples were compressed in vertical direction to failure and the shear strength of the material was determined. The tests were made in following steps:

- Small samples were compacted at a pressure of ~25 MPa (Ø 35 mm, h 70 mm).
- A sample was placed in a load frame and was compressed by applying a vertical constant deformation rate of ~0.09 mm/min with continuous measurement of the vertical load and the deformation of the sample (see Figure 4-1).
- The shear strength of the sample was evaluated according to Equation 4-1.

$$\sigma_{max} = \frac{P_{max}}{A} \tag{4-1}$$

where
σ_{max} = Maximum Deviator stress (kPa)
A = Area of the sample (m)
P_{max} = Maximum applied vertical load (kN)

Results from the measurements made on Friedland are shown in Figure 4-2. Corresponding plots for ASHA 230 and 30/70-mixtures are shown Appendix 2. The results from the tests are summarized in Table 4-1. Altogether four tests were performed on each material. Three of the tests were made on samples with the expected block density while one test was made on sample with a somewhat lower density (Test No 8, 12 and 16). The largest variation in the measured maximum deviator stress and the strain at failure was measured for the 30/70 mixture. The reason for this might be the small dimensions of the samples compared to the maximum grain size of the ballast material. Another explanation might be related to the difficulties to get homogeneous samples. The highest maximum deviator stress was measured for the Friedland clay.

The Young's modulus are also evaluated from the tests and reported and in Table 4-1. The evaluated moduli are in the same range as those presented in Table 3-1 except for the 30/70-mixture. The discrepancy is probably caused by the variation in density for the samples.

Figure 4-1. *Test arrangement for determination of the shear strength of pre-compacted samples of backfill material.*

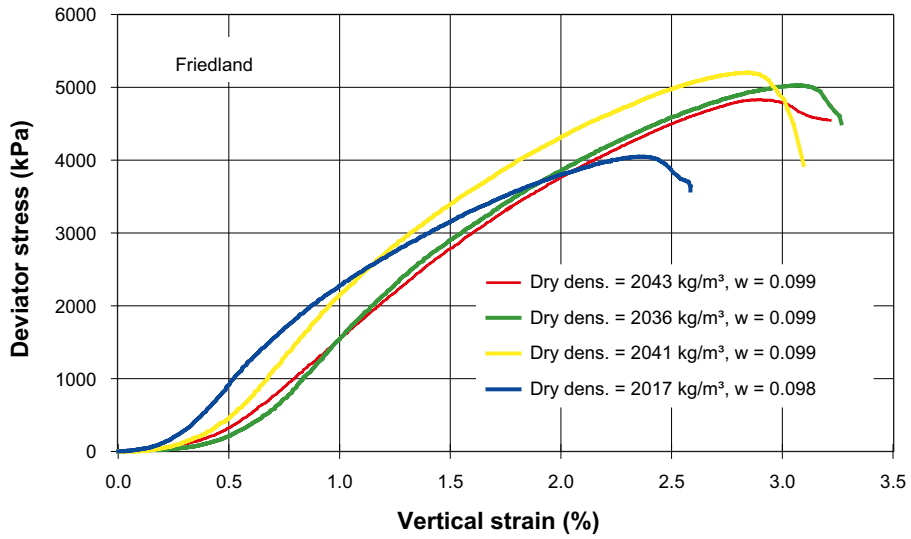

Figure 4-2. *Data from unconfined one dimensional compression tests made on the Friedland clay.*

Table 4-1. The maximum deviator stress and the strain at failure evaluated from unconfined one dimensional compression test made on the investigated backfill materials.

Test No	Mtrl	Dry density (kg/m³)	Water ratio	Max Dev stress (kPa)	Strain at failure (%)	E-modulus (MPa)
5	Asha 230 B	1,698	0.170	3,571	2.1	240
6	Asha 230 B	1,698	0.170	3,496	2.1	235
7	Asha 230 B	1,707	0.168	3,660	2.1	235
8	Asha 230 B	1,632	0.168	2,301	1.8	160
9	Friedland	2,043	0.099	4,827	2.9	255
10	Friedland	2,036	0.099	5,027	3.1	315
11	Friedland	2,041	0.099	5,200	2.8	325
12	Friedland	2,017	0.098	4,046	2.4	305
13	30/70 mix	2,192	0.056	4,262	2.1	410
14	30/70 mix	2,195	0.051	4,060	1.8	535
15	30/70 mix	2,181	0.055	4,904	1.6	630
16	30/70 mix	2,133	0.051	2,626	1.8	300

4.2 Beam tests

With the second type of test the tensile strength of samples of backfill material has been determined. The tests were performed as follows:

- Small samples were compacted at a pressure of ~25 MPa (Ø 50 mm, h 20 mm).
- Beams were sawn from the samples (axbxc ~10×20×35 mm³).
- The beam was bended by applying a constant deformation rate of about 0.10 mm/min at the middle of the beam. The load and the displacement was measured continuously (see Figure 4-3).
- The tensile stress (σ_t) and the strain (ε_t) were evaluated with the following equations (see also Appendix 5).

$$\sigma_t = \frac{6Qc}{4ba^2} \tag{4-2}$$

$$\varepsilon_t = \frac{a\omega 6}{c^2} \tag{4-3}$$

where
Q = vertical force
a = sample height
b = sample width
c = the length between the support points
ω = the vertical displacement at the middle of the beam

Results from the beam tests made on Friedland clay are shown in Figure 4-3: Corresponding plots for ASHA 230 are shown in Appendix 3. The results from the tests are summarized in Table 4-2. Four of the tests (Test 1–4, ASHA 230) were made on samples with relatively low densities while the rest of the tests were made on samples with the expected block density. The tests made on 30/70-mixture did not yield reliable results due to preparation problems. The compacted samples were very brittle which made it difficult to saw out a small beam. The results from the tests made on 30/70-mixture are not reported here.

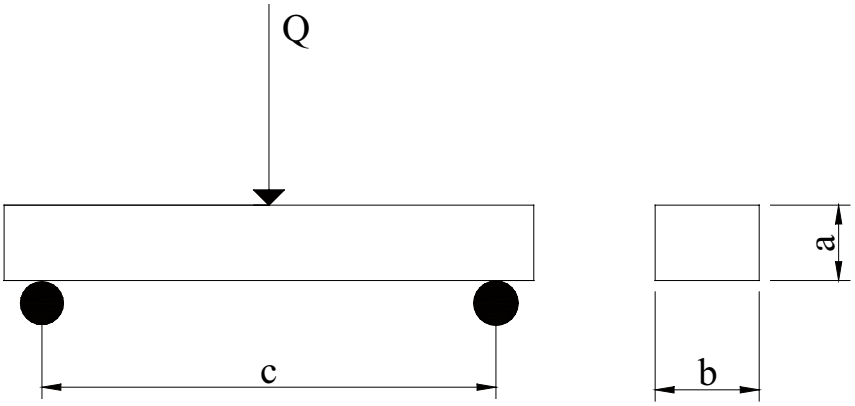

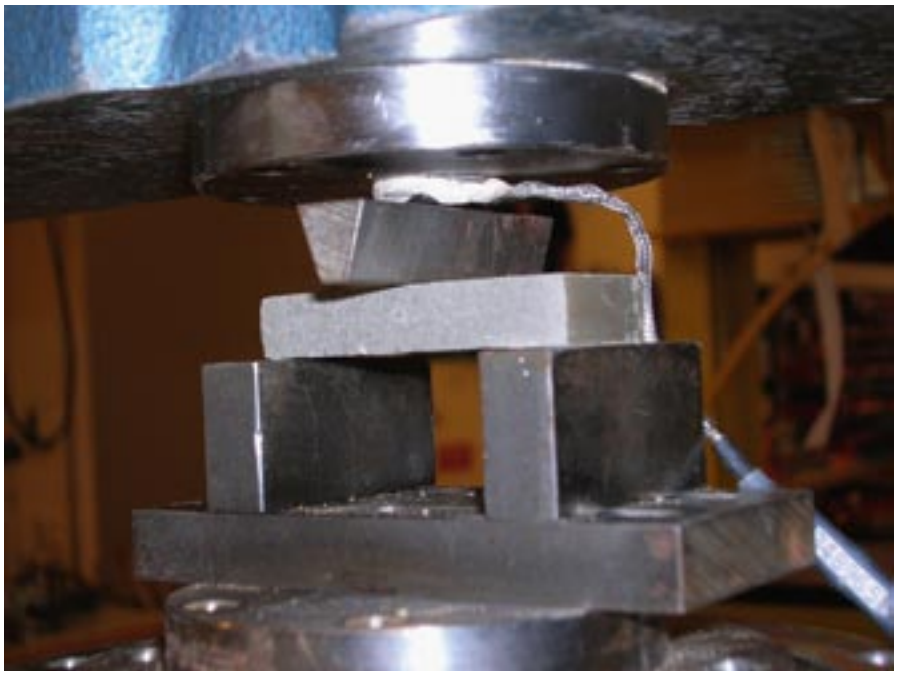

Figure 4-3. *Test arrangement for determination of the tensile strength.*

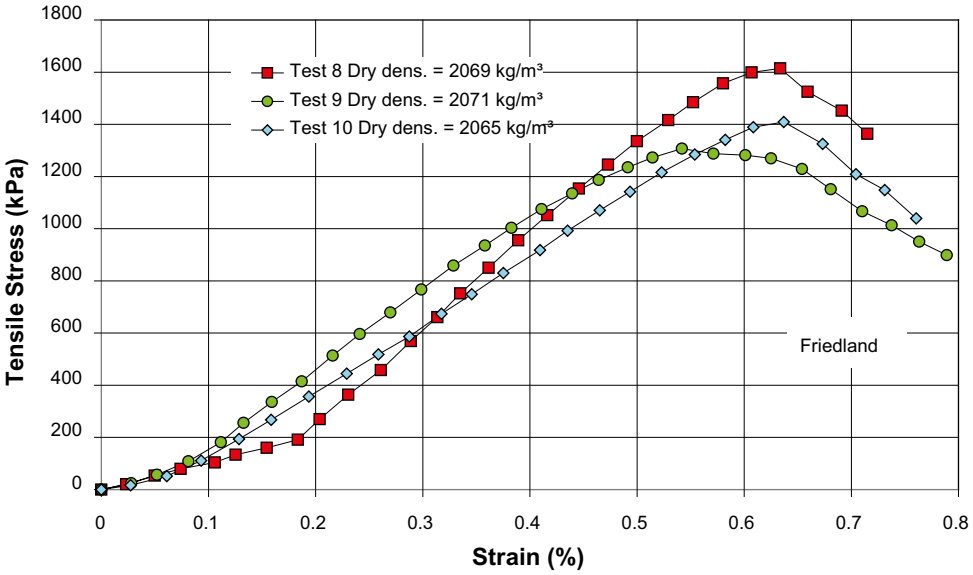

Figure 4-4. *Data from beam tests made on Friedland clay.*

Table 4-2. Maximum tensile stress and strain at failure evaluated from beam tests.

Test No	Mtrl	Dry density (kg/m³)	Water ratio	Max Tensile stress (kPa)	Strain at failure (%)
1	Asha 230 B	1,681	0.162	612	0.68
2	Asha 230 B	1,672	0.164	600	0.91
3	Asha 230 B	1,673	0.163	528	0.53
4	Asha 230 B	1,671	0.161	504	0.74
5	Asha 230 B	1,692	0.173	722	0.57
6	Asha 230 B	1,741	0.171	820	0.61
7	Asha 230 B	1,725	0.171	996	0.70
8	Friedland	2,069	0.098	1,615	0.63
9	Friedland	2,071	0.097	1,307	0.54
10	Friedland	2,065	0.098	1,409	0.64

5 Compression properties of unsaturated filling of bentonite pellets filling

With the concept of backfilling the tunnels with pre-compacted blocks the slot between the blocks and the rock surface in the tunnel will be filled with pellets of bentonite. It is of importance to know the compression properties of the clay pellets filling in order to be able to calculate the deformation of the filling caused by the swelling of the buffer in the deposition hole (see Section 6). The compression properties were investigated with oedometer tests in a large Rowe oedometer, see Figure 5-1 and also in Proctor cylinders. The test has been performed as follows:

- The oedometer (Ø 250 mm, h 80 mm) was filled with bentonite pellets to an initial dry density.
- A vertical load was applied on the pellets in steps up to 800 kPa and the deformation of the pellets filling was measured continuously.
- The dry density of the pellets filling was determined as function of the applied load with the use of the measurements made of the vertical displacement

The results for the tests made on pellets of MX-80 (made in the Rowe oedometer Test 1 and Test 2) are plotted in Figure 5-2. The initial conditions of the pellets are shown in the figure.

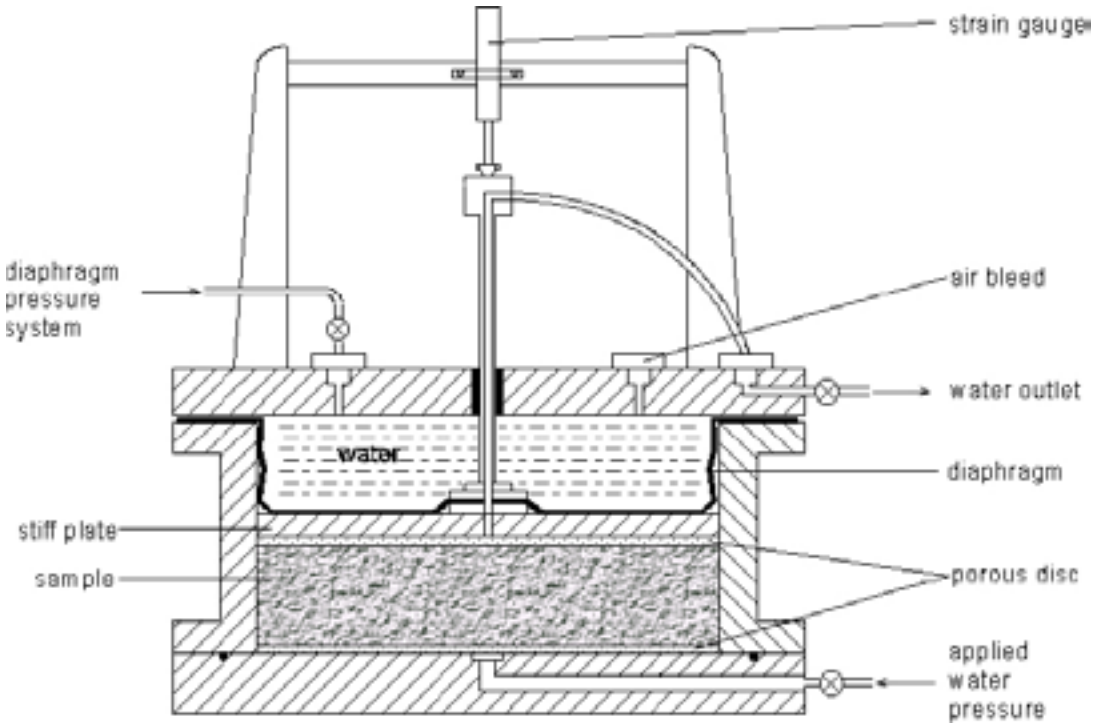

Figure 5-1. *A Rowe oedometer for determining the compressibility of the unsaturated pellets filling.*

In addition to the tests performed in the Rowe oedometer, one test on MX-80 pellets was made in a rigid oedometer (with the height of about 87 mm and a diameter of about 101 mm.) where the pellets where compacted up to a pressure of about 5,000 kPa at a constant rate of strain. The results form this test are also plotted in Figure 5-2 (Test 3). The test made in the proctor cylinder is indicating a somewhat stiffer behavior compared to the tests made in the Rowe oedometer. The Minelco, Friedland and Cebogel pellets/granules were also tested in the proctor cylinder up to a pressure of about 500 kPa and the results from the tests are also plotted in Figure 5-2. The figure shows that when loading the samples up to 5,000 kPa the highest compression was measured on the Friedland while the lowest compression was measured for the Minelco material.

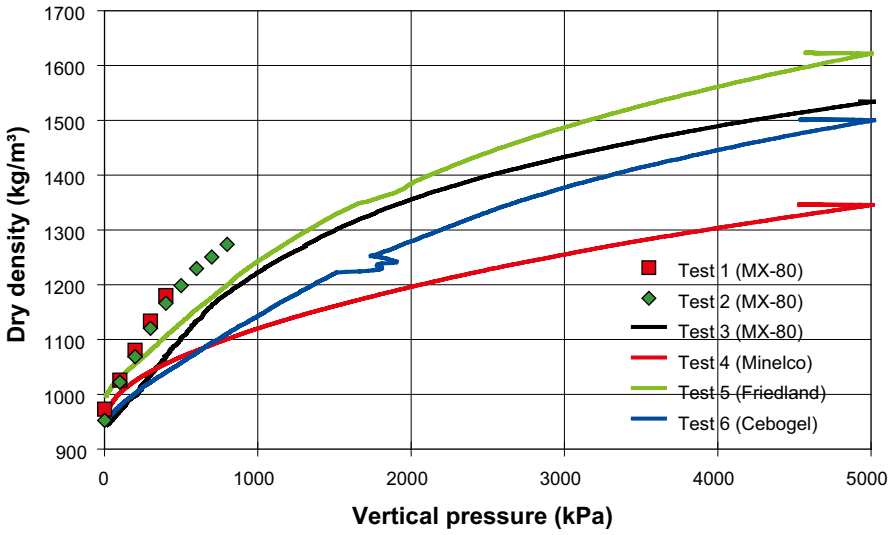

Test No	*Water ratio*	*Init. dry density*
	(%)	*(kg/m³)*
1	*13.0*	*970*
2	*13.0*	*950*
3	*11.5*	*940*
4	*16.5*	*970*
5	*7.0*	*1000*
6	*19.5*	*960*

Figure 5-2. *The dry density as function of the applied vertical stress for tests made with pellets of MX-80, Minelco, Friedland and.Cebogel. Test 1 and 2 are made in a Rowe oedometer while the rest of the tests are made in a proctor cylinder.*

6 Calculations of the compression of unsaturated backfill

When the buffer material in the deposition hole is wetted and saturated it causes a pressure on the backfill that can be more or less wetted. In the previous phase of the BACLO program the compression of the backfill in the tunnel were calculated assuming a fully saturated and homogenized backfill. In this phase of the program the other extreme was investigated by calculating the compression of the clay backfill of pre-compacted blocks and pellets. The calculations were made for three backfill materials, Friedland, Asha 230 and 30/70 mixture of ballast and Deponit CAN. The calculations were made in the following way:

1. The same type of calculations as in phase 2 but elastic parameters of the backfill blocks and pellets are used for describing the properties of the backfill. In these calculations the backfill is modeled as a continuum material. The compression of the backfill is compared with the swelling of the buffer in the deposition hole. The outcomes of the calculations are the final compression of the backfill and the density of the buffer in the deposition hole.
2. Simplified calculations where the filling of the tunnel is consisting of pre-compacted blocks of backfill material and bentonite pellets/granules placed between the blocks and the rock surface.

6.1 Calculations assuming the backfill to be continuum material

In chapter 3 the elastic parameters (E-modulus, ν) of the different backfill materials were determined. A compression modulus (M) of the backfill blocks and the vertical strain (ε) resulting from an applied stress can be calculated as:

$$M = E \times \frac{1-\nu}{(1+\nu)\times(1-2\nu)} \tag{6-1}$$

$$\varepsilon = \frac{\Delta\sigma}{M} \tag{6-2}$$

where
ν = Poison ratio
E = Young's modulus (kPa)
M = "Oedometer" modulus (kPa)
Δσ = vertical stress in the backfill due to the swelling pressure of the buffer (kPa)

A simplified calculation of the compression of the backfill above a deposition hole due to the swelling of the buffer in a KBS-3 tunnel can be made based on a theory presented in /6-1/. The compression of the backfill material depends on the following factors:

1. Deformation properties of the backfill (Equation 6-1).
2. The friction between the buffer and the rock surface in the deposition hole.
3. The void ratio and the resulting swelling pressure of the buffer.
4. The stress distribution in the backfill material.
5. The dimensions of the deposition hole and the tunnel.

The following assumptions were made:

- The deposition hole has a radius of 0.875 m and the thickness of the buffer above the canister is 1.50 m. The thickness of the backfill inside the deposition hole is 1.00 m. The tunnel has a total height of 5.4 m (see Figure 6-1).
- There is no friction between the backfill material and the rock in the deposition hole.
- The void ratio of the buffer is a function of the swelling pressure according to Equation 6-3 (This empiric relation is described in detail in /6-2/. The relation is based on swelling pressure measurements on MX-80):

$$e = e_0 \times \left[\frac{p}{p_0}\right]^{\beta} \qquad (6\text{-}3)$$

where
e_0 = void ratio at the reference pressure p_0
e = void ratio at the pressure p
p_0 = reference pressure (= 1,000 kPa)
β = pressure exponent (=–0.19)

- The reduced swelling pressure at the buffer/backfill interface due to the friction between the buffer and the rock (see Figure 6-2) can be calculated according to Equation 6-4. (This relation is described in detail /6-1/. See also Appendix 6):

$$P_{sa} = P_{sb} \times e^{-\left(\frac{2z\tan(\phi)}{r}\right)} \qquad (6\text{-}4)$$

where
P_{sa} = swelling pressure in the interface between the buffer and the backfill
P_{sb} = initial swelling pressure of the buffer
r = radius of the deposition hole (= 0.875 m)
ϕ = friction angle between the buffer and the rock surface of the deposition hole
z = vertical distance from the buffer/backfill interface

- The bentonite buffer above the canister is so thick that the buffer around the canister is not involved in the swelling.
- The vertical stress in the backfill in the deposition hole is constant.
- The vertical stress distribution in the backfill above the deposition hole (in the tunnel) are calculated according to the theory by Boussinesq (elastic theory):

$$\Delta\sigma = q \times \left[1 - \left(\frac{1}{1 + (r/y)^2}\right)^{3/2}\right] \qquad (6\text{-}5)$$

where
$\Delta\sigma$ = vertical stress in the backfill due to the swelling pressure of the buffer
q = swelling pressure of the buffer
r = radius of the deposition hole (= 0.875 m)
y = distance from tunnel floor to the position were the stress is calculated

Equation 6-5 is assuming that the backfill material is homogeneous and elastic which might be questionable for a filling built up by pre-compacted blocks. The total compression of the backfill and the pellets is assumed to consist of three parts: the settlement of the blocks itself, the settlement of the pellets filling close to the sealing of the tunnel and the deformation of the slots between the blocks.

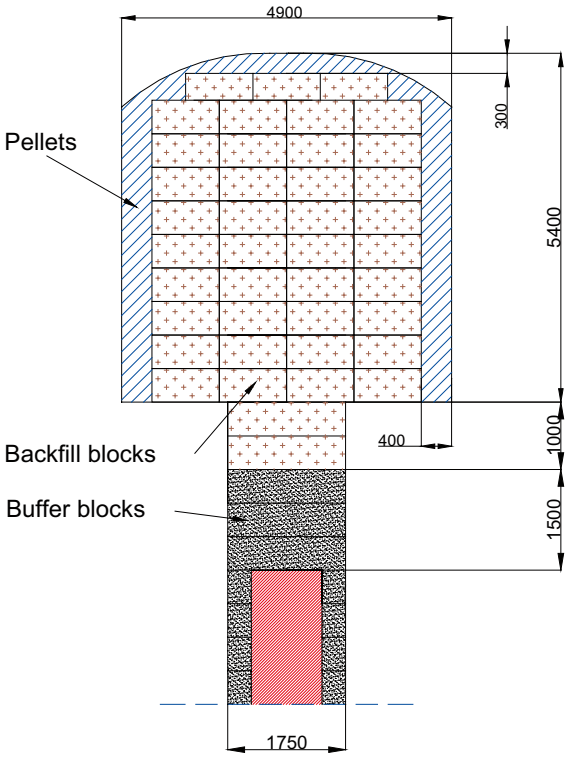

Figure 6-1. *Geometry of tunnel backfilled with blocks and pellets.*

With these equations the maximum deformation (compression) of the backfill can be calculated in the following steps:

A. The backfill above the buffer is divided in layers with defined thickness. The increase in vertical stress at the centre of each layer caused by the swelling pressure of the buffer is calculated with Equation 6-5. Knowing this increase in stress the strain for the centre of each layer can be calculated with Equation 6-2. By assuming that the change in void ratio at the centre of the layers is valid for the whole layer, the total compression of the block filling can be calculated as the sum of the compression of all the layers.

B. The deformation of the pellet filling close to the ceiling of the tunnel is calculated in the same way as for the filling of blocks. The increase of the vertical stress in the pellets filling is calculated with Equation 6-5 and the change in dry density is calculated with the use of the modulus determined from Figure 5-2.

C. Maximum 4 mm slots caused by differences in heights of the backfill blocks are expected. Since such slots occur over a limited part of the horizontal joints, due to the overlapping brick work, they will only partially be closed. It is conservatively assumed here that the entire slot apertures will be closed. Altogether there are 9 such joints (see Figure 6-1), which yields the following total displacement:

$\delta_s = a_{s1} \cdot N = 0.036$ m

where
a_{s1} = aperture of one slot
N = number of slots

D. Knowing the friction angle between the buffer and the wall of the deposition hole the pressure P_{sa} (see Figure 6-2) can be calculated with Equation 6-4. (P_{sb} is assumed to be 7,000 kPa which corresponds to a saturated density of the buffer of 2,011 kg/m^3). The change in swelling pressure from Psb to Psa causes changing in void ratio of the buffer which can be calculated with Equation 6-3. With the known volume of the zone where the swelling occurs and the average change in void ratio the swelling of the buffer can be calculated.

E. The final compression of the backfill can be evaluated at the inter-section between the deformation curve of the backfill (sum of deformation from A, B and C) and the swelling curve of the buffer material (see Section 6.3).

6.2 Calculations assuming the backfill is consisting of bricks placed as a pillar over the deposition hole

An alternative view is to assume that the entire force is taken only by the blocks located above the deposition hole and that there is no lateral stress distribution. The motivation for such an approach is that there are vertical slots between the blocks and that there is a large pellets filled slot on both sides of the block staple, which will allow horizontal deformations and prevent lateral stress propagation. The total deformation can be calculated in the same way as shown in Section 6.1 with the exception that the deformation of the blocks and the pellets close to the ceiling are calculated as follows:

A'. The elastic deformation of the blocks above the buffer is calculated with the following equation.

$$s_b = \frac{\sigma}{E} \times h_b \qquad (6\text{-}6)$$

where
s_b = deformation of the blocks
σ = the swelling pressure from the buffer (= 7,000 kPa)
h_b = the height of the pillar of blocks (= 6.1 m see Figure 6-1)
E = the Young's modulus of the blocks (see Table 3-1)

B'. The deformation of the pellets filling close to the sealing can be calculated from the measurements of the compression of the pellets (see Figure 5-2). The figure indicates that at an increase of the vertical load from 0 to 7,000 kPa the dry density increases from ρ_{di} = 950 kg/m^3 to ρ_{dc} = 1,570 kg/m^3. The deformation of the pellets can then be calculated with the following equation.

$$s_{pellets} = (1 - \frac{\rho_{di}}{\rho_{dc}}) \times h_p = (1 - \frac{950}{1570}) \times 0.3 = 0.118m \qquad (6\text{-}7)$$

where
$s_{pellets}$ = deformation of the pellet filling
ρ_{di} = the initial dry density of the pellets (= 950 kg/m^3)
ρ_{dc} = the dry density of the pellets at the vertical stress 7,000 kPa (= 1,570 kg/m^3)
h_p = the height of the pellets filling (= 0.3 m, see Figure 6-1)

The used equation for determining the compression of the pellets filling is assuming that no vertical deformation in the filling is occurring. Furthermore the equation is assuming a linear relation between the dry density of the filling and the applied load. These assumptions are underestimating the deformation of the pellets filling.

The final compression of the backfill can be evaluated at intersection between the deformation curve of the backfill (sum of deformation from A', B' and C) and the swelling curve of the buffer material (see Section 6.3).

6.3 Results from the calculations

Figure 6-3 shows the results from the calculation where the backfill materials of blocks are modelled as continuum materials. The compression of the backfill materials and the swelling of the buffer are plotted as function of the vertical stress of the buffer and the backfill at the buffer/backfill interface. The swelling of the buffer is plotted with four different assumptions of the friction between the rock surface of the deposition hole and the buffer.

Except for the maximum compression/swelling, the distance between the buffer/backfill interface and the level in the deposition hole where no reduction in the swelling pressure occurs is calculated (the distance z in Figure 6-2). The swelling pressure (P_{sa}) at the interface between the buffer and the backfill can also be calculated. Furthermore the density at the lid of the canister and at the interface between buffer and backfill are determined from the calculated swelling pressure. These parameters are shown in Table 6-1 for the case of 10º friction angle between buffer and rock surface. The distance z should according to the assumptions for the requirements be smaller than 1.5 m (the thickness of bentonite on top of the canister). This is not the case for any of the investigated backfill materials. However the calculated saturated densities close to the canister lid are higher than 1,950 kg/m^3 which is the lower limit for the requirement of the buffer density.

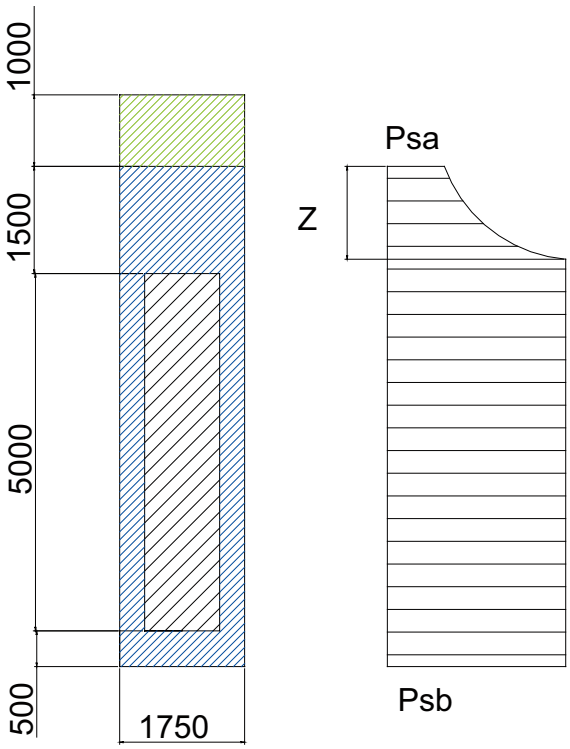

Figure 6-2. *A schematic drawing of the stresses in the buffer according to Equation 6-4.*

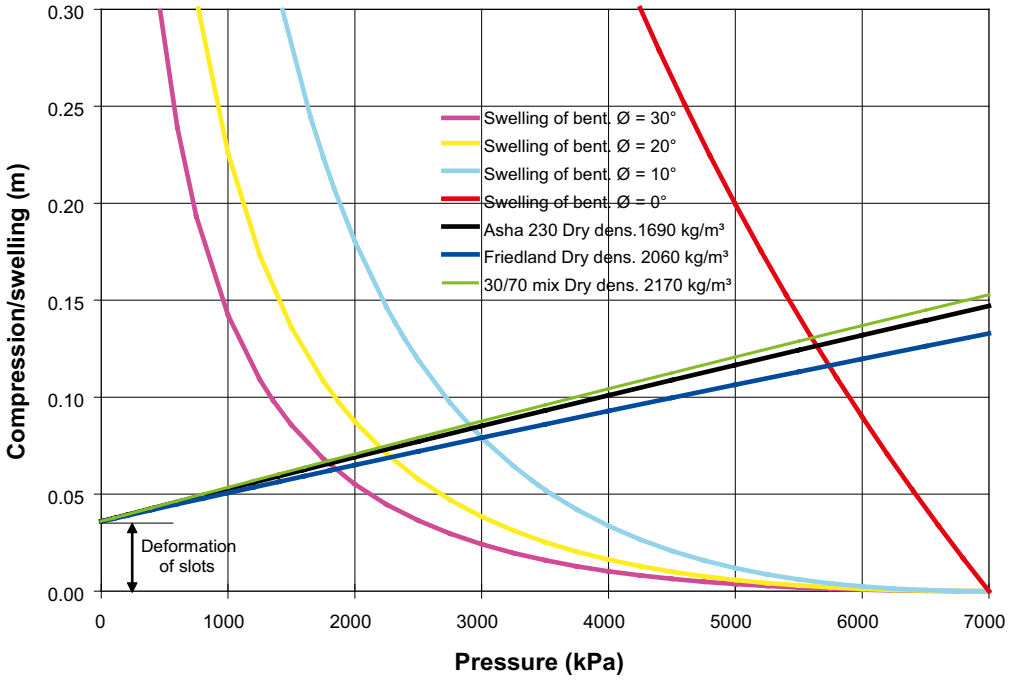

Figure 6-3. *The displacement of the interface between the compacted bentonite and the overlaying backfill modelled as continuum materials. The calculations are made at different angles of friction between the buffer and the surface of the deposition hole and with the assumed achievable density of the blocks.*

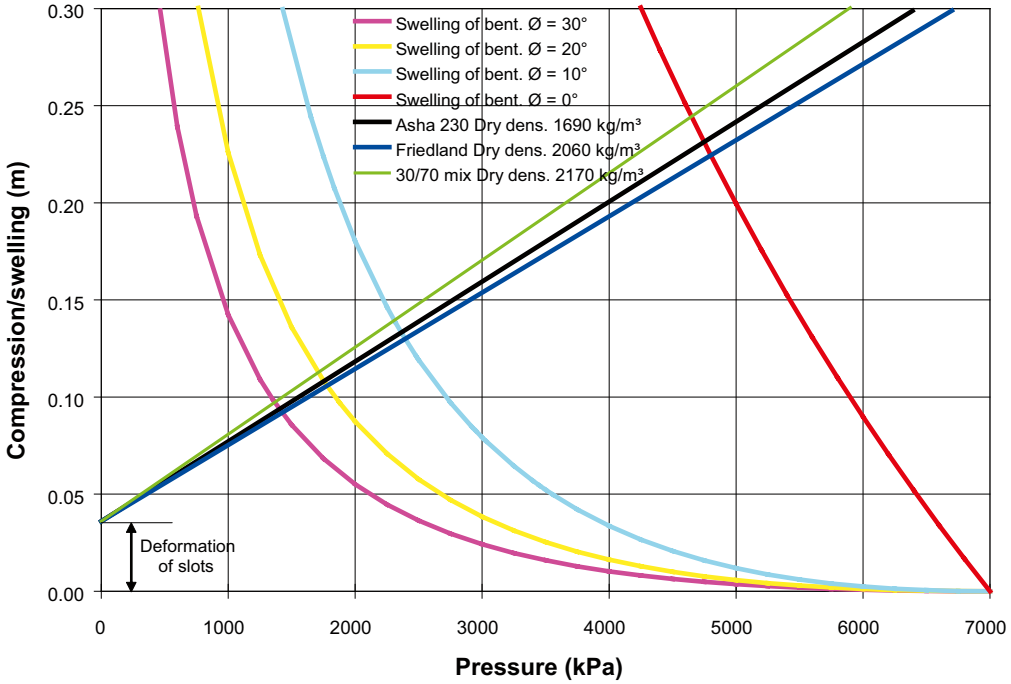

Figure 6-4. *The displacement of the interface between the compacted bentonite and the overlaying backfill modelled as a pillar of blocks above the buffer. The calculations are made at different angles of friction between the buffer and the surface of the deposition hole and with the assumed reachable density of the blocks.*

Table 6-1. Results from the calculations of the compression of the backfill materials. The calculations are made with the assumption of a friction angle of 10º between the buffer and the rock surface in the deposition hole.

Material	Concept	Initial dry dens. blocksl (kg/m^3)	Compression (m)	Psa (kPa)	Z (m)	Saturated buffer density at canister lid (kg/m^3)	buffer/backfill (kg/m^3)
Asha 230 B	Continuum	1,690	0.083	2,950	2.144	1,990	1,940
Friedland	Continuum	2,060	0.078	3,000	2.102	1,990	1,940
30/70	Continuum	2,170	0.085	2,920	2.169	1,990	1,940
Asha 230 B	Blocks	1,690	0.133	2,370	2.687	1,970	1,920
Friedland	Blocks	2,060	0.130	2,395	2.661	1,970	1,920
30/70	Blocks	2,170	0.139	2,315	2.745	1,970	1,920

7 Risk of failure

Since the lateral support from the side exerted blocks and pellets is expected to be low for the case when the saturation of the backfill is low and the buffer in the deposition hole is saturated there might be a risk of mechanical failure of a block column above a deposition hole. The block column may be considered equivalent to a large cylinder with a diameter 1.75 m and the height 5.1 m. Assuming no lateral support the deviator stress for the cylinder will be the swelling pressure from the buffer. According to Table 6-1 the expected swelling pressure varies between 2,300 and 2,400 kPa depending on the assumption made about the compression of the backfill while the variations between the different block materials are small. The swelling pressure is then compared with the maximum deviator stresses from the unconfined laboratory test, see Table 4-1. The lowest deviator stress was measured for the blocks of ASHA 230 (about 3,500 kPa for the samples with the expected block density). The comparison indicates that the safety margin for failure is small.

8 Measurements of hydraulic conductivity and swelling pressure

In the previous phase of this project the hydraulic conductivity and swelling pressure were measured on several backfill materials in order to find out the requirements on density for reaching a swelling pressure of 200 kPa and a hydraulic conductivity of 1E–10 m/s /1-3/. These evaluated densities are however very low compared to the densities expected in a filling consisting of pre-compacted blocks (corresponding to ~80% block filling degree). Therefore additional oedometer tests have been performed on three materials, Asha 230, Friedland and 30/70-mixture.

The hydraulic and swelling pressure tests were made in oedometers with a diameter of 50 mm. The height of the samples was 20 mm. The tests were prepared and made in the following steps:

- The sample was compacted into the oedometer (see Figure 8-1) to a specified dry density at the initial water ratio of the material (see Table 2-1).
- A piston was placed on top of the sample and the sample was saturated from both the top and bottom filters during continuous measurement of the occurring swelling pressure, with the load cell placed on top of the piston. The tests were performed with two different water salinities (3.5% and 7%)
- After saturation, a pore pressure gradient was applied over the sample and the volume of outflowing water measured. This volume was used for calculating the hydraulic conductivity of the sample. The gradient during the tests was about 2,000 (corresponding to a pore pressure difference over the sample of Δu = 400 kPa) for the test made with Asha 230 and Friedland and about 500 (Δu = 100 kPa) for the tests made with 30/70 mixture. All the test were made with a backpressure of 100 kPa.
- The sample was pressed out of the oedometer after the test and its water ratio and density were determined.
- The swelling pressure and the hydraulic conductivity for the different materials are presented as function of the dry density.

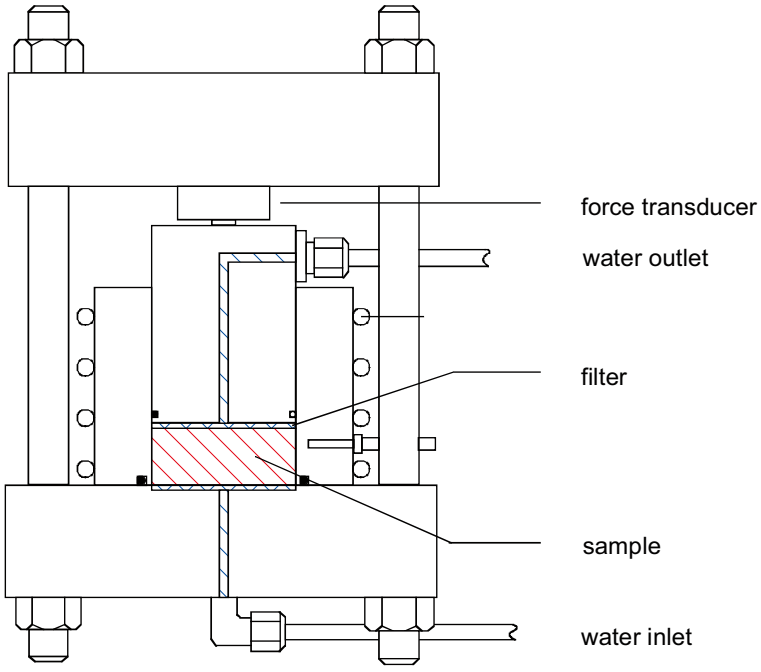

Figure 8-1. *A schematic drawing of an oedometer.*

8.1 Results from the measurements

The measured swelling pressure and hydraulic conductivity of the Friedland clay are plotted in Figure 8-2 and Figure 8-3 together with results from previous measurements made on samples with lower densities. Corresponding plots for the two other backfill materials are given in Appendix 4. Table 8-1 shows the evaluated swelling pressure and hydraulic conductivity at the expected dry density.

Table 8-1. Results from the evaluation of the hydraulic conductivity and swelling pressure of the different backfill materials. The evaluations are made at expected density of the backfill materials at different water salinity ($NaCl:CaCl_2$, 50:50).

Material	Dry density (kg/m³)	Salinity (%)	Hydr. cond. (m/s)	Swelling pressure (kPa)
Asha 230 B	1,540	3.5	8.0E–13	10,000
Asha 230 B	1,540	7	8.0E–13	7,500
Friedland	1,780	3.5	2.0E–12	1,500
Friedland	1,780	7	2.0E–12	1,500
30/70	1,910	3.5	3.0E–11	700
30/70	1,910	7	3.0E–11	500

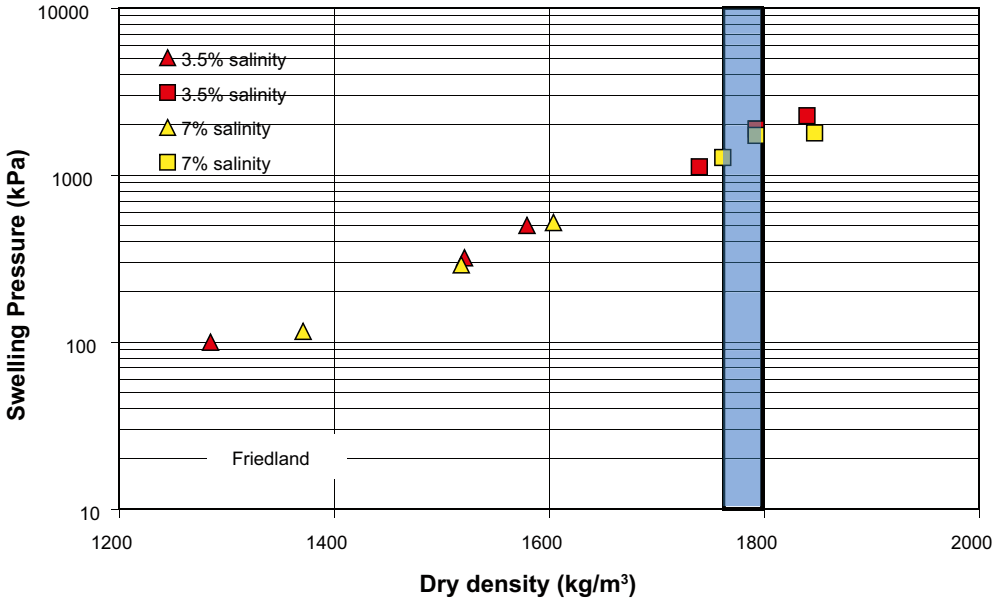

Figure 8-2. The swelling pressure plotted as function of the dry density for Friedland clay. The measurements are made with water salinity 3.5% and 7%. The shaded part of the plot is representing the expected average density of the backfill when using pre-compacted blocks.

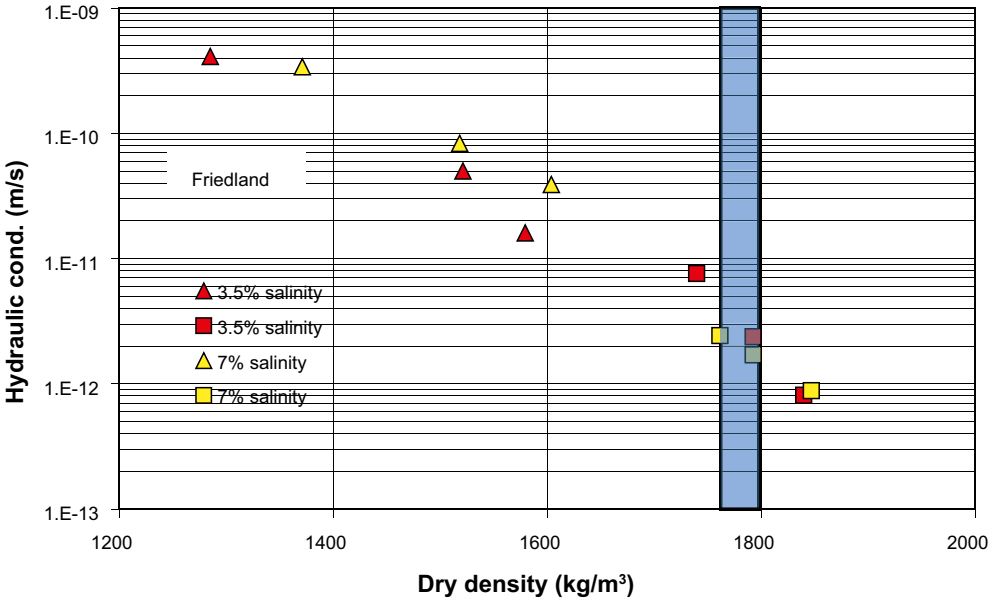

Figure 8-3. *The hydraulic conductivity plotted as function of the dry density for Friedland clay. The measurements are made with water salinity 3.5% and 7%. The shaded part of the plot is representing the expected average density of the backfill when using pre-compacted blocks.*

9 Comments and conclusions

The strength of the materials evaluated from unconfined one dimensional compression tests on samples compacted with 25 MPa compaction pressure show that the Friedland samples had the highest unconfined compressive strength of about 5,000 kPa.

The tensile strength of the materials evaluated from beam test gave not reliable values for the 30/70 mixture because of the difficulties to saw out samples from the compacted material. The measured tensile strength for Frieldand was about 1,450 kPa while the measured strength of ASHA 230 was about 850 kPa.

The compressibility measured on three different “pellet fillings” show a variation between the materials. The highest compressibility was measured for Friedland clay granules while Minelco granules were the stiffest material.

Calculations of compression of not wetted backfill, consisting of pre-compacted blocks and pellet filling, were made with two different assumptions about the backfill. At the first type of calculations the backfill was assumed to be a continuum material while at the second type the backfill was modelled as a pillar of blocks piled on top of the buffer in the deposition hole. The second model gave the largest compression of the backfill, about 0.140 m. The differences in the calculated compression between different materials were very small.

The calculation of the compression of the backfill was made in steps where the swelling of the buffer and the compression of the backfill was set to be equal. The calculations of the deformations were made with simple methods and with several assumptions. The results should be validated with other methods e.g. FE calculations.

The hydraulic conductivities evaluated at the expected dry density after saturation in a backfilling composed of pre-compacted blocks and pellets were much lower than 1E–10 m/s for the three investigated materials. This is valid for both types of used water.

The swelling pressures evaluated at the expected dry density after saturation in a backfilling composed of pre-compacted blocks and pellets were higher than 200 kPa for the three investigated materials. This is valid for both types of used water.

10 References

/1-1/ **Gunnarsson D, Morén L, Sellin P, Keto P, 2006.** Deep repository – engineered barrier systems. Assessment of backfill materials and methods for deposition tunnels. SKB R-06-71, Svensk Kärnbränslehantering AB.

/1-2/ **Gunnarsson D, Börgesson L, Keto P, Tolppanen P, Hansen J, 2004.** Backfilling and closure of the deep repository. Assessment of backfill concepts. SKB R-04-53, Svensk Kärnbränslehantering AB.

/1-3/ **Johannesson L-E, Nilsson U, 2006.** Deep repository – engineered barrier systems. Geotechnical behaviour of candidate backfill materials. Laboratory tests and calculations for determining performance of the backfill. SKB R-06-73, Svensk Kärnbränslehantering AB.

/2-1/ Konsistensgränser. Förslag till geotekniska laboratorieanvisningar, del 6. Byggforskningens informationsblad B11:1974 (in Swedish).

/2-2/ **Keto P, Kuula-Väisänen P, Ruuskanen J, 2005.** Effect of material parameters on the compactibility of backfill materials. Posiva Working report 2006-34.

/6-1/ **Börgesson L, 1982.** Prediction of the behaviour of the bentonite-based buffer materials. SKBF/KBS Stripa Project 82-08.

/6-2/ **Börgesson L, Johannesson L-E, Sandén T, Hernelind J, 1995.** Modelling of the physical behaviour of water saturated clay barriers. Laboratory tests, material models and finite element application. SKB TR 95-20, Svensk Kärnbränslehantering AB.

Appendix 1

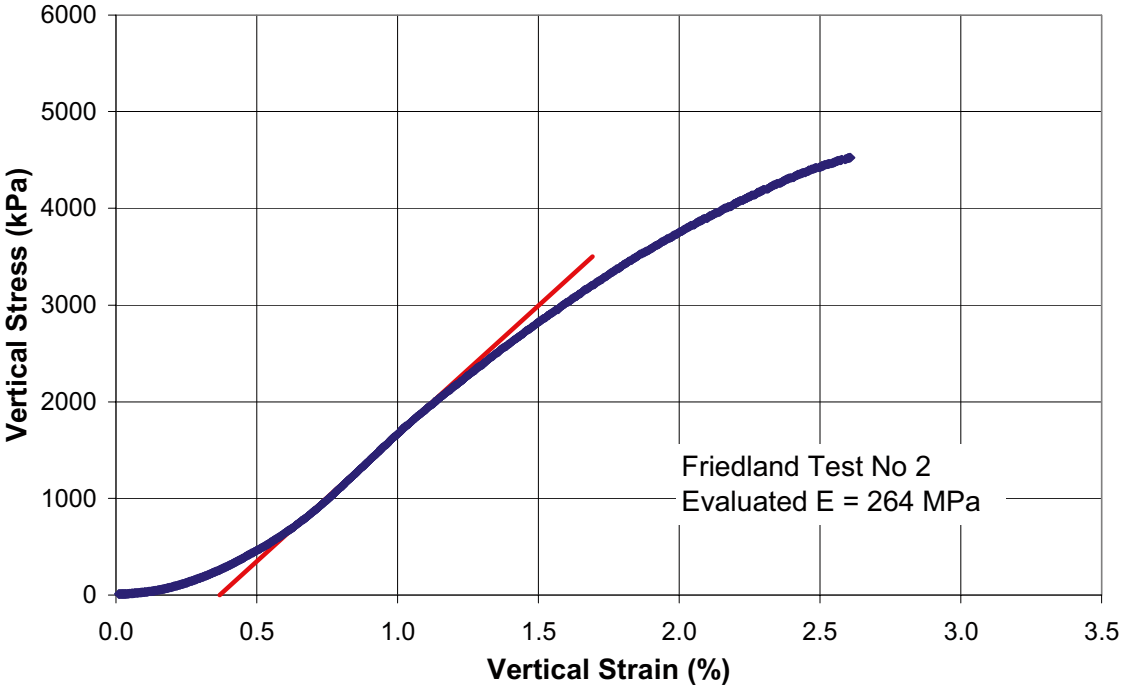
6000
5000
4000
3000
2000
1000
0
Vertical Stress (kPa)
0.0
0.5
1.0
1.5
2.0
2.5
3.0
3.5
Vertical Strain (%)
Friedland Test No 2
Evaluated E = 264 MPa

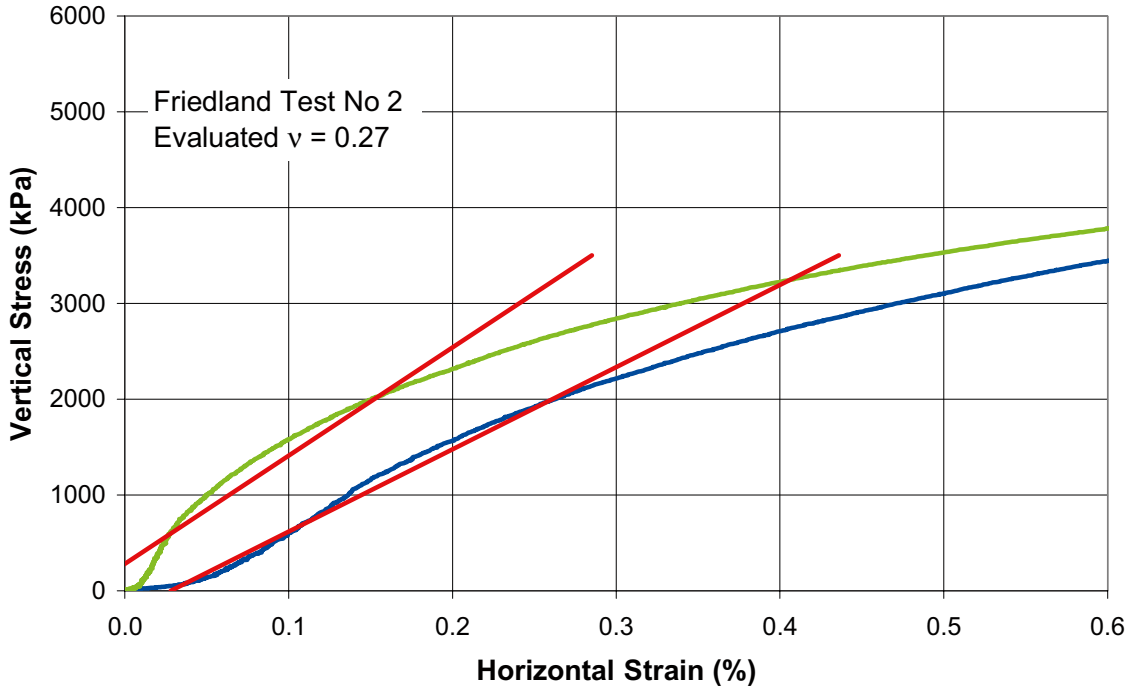
6000
5000
4000
3000
2000
1000
0
Vertical Stress (kPa)
0.0
0.1
0.2
0.3
0.4
0.5
0.6
Horizontal Strain (%)
Friedland Test No 2
Evaluated ν = 0.27

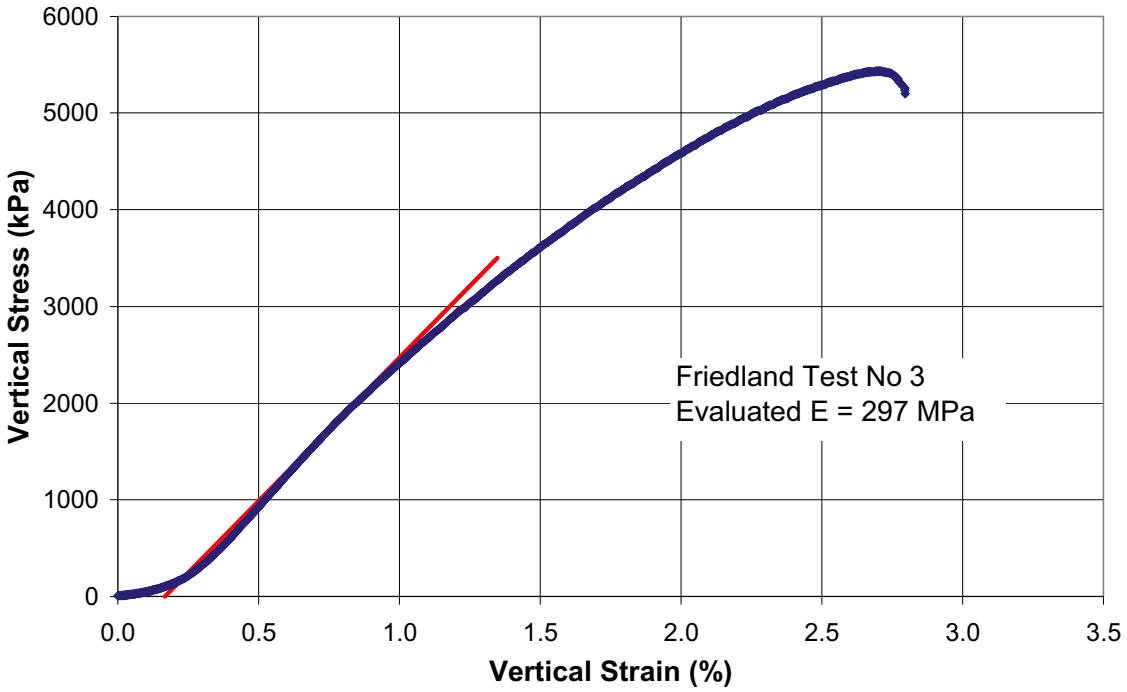
6000
5000
4000
3000
2000
1000
0
Vertical Stress (kPa)
0.0
0.5
1.0
1.5
2.0
2.5
3.0
3.5
Vertical Strain (%)
Friedland Test No 3
Evaluated E = 297 MPa

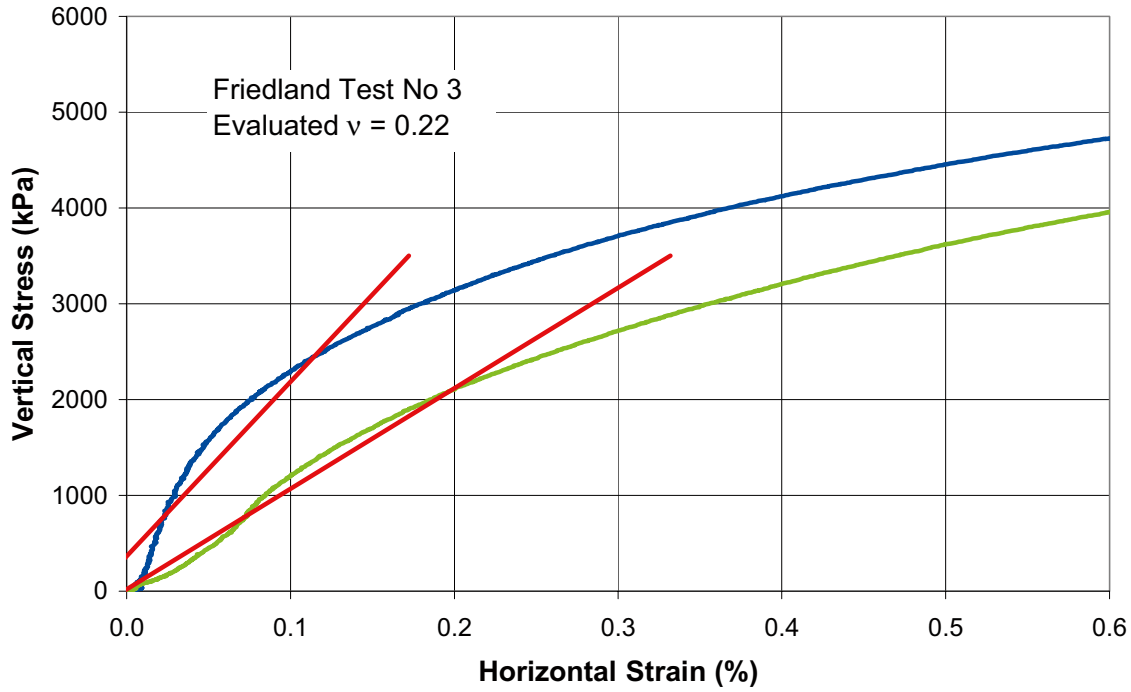
6000
5000
4000
3000
2000
1000
0
Vertical Stress (kPa)
0.0
0.1
0.2
0.3
0.4
0.5
0.6
Horizontal Strain (%)
Friedland Test No 3
Evaluated ν = 0.22

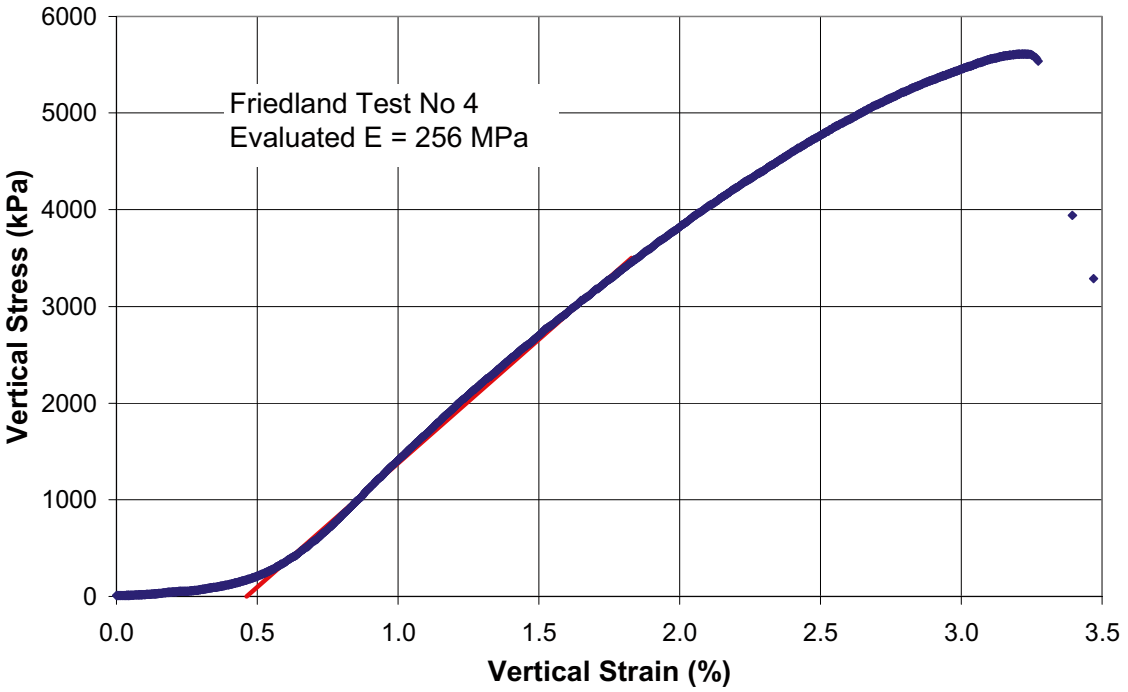
Friedland Test No 4
Evaluated E = 256 MPa
Vertical Stress (kPa)
Vertical Strain (%)
6000
5000
4000
3000
2000
1000
0
0.0
0.5
1.0
1.5
2.0
2.5
3.0
3.5

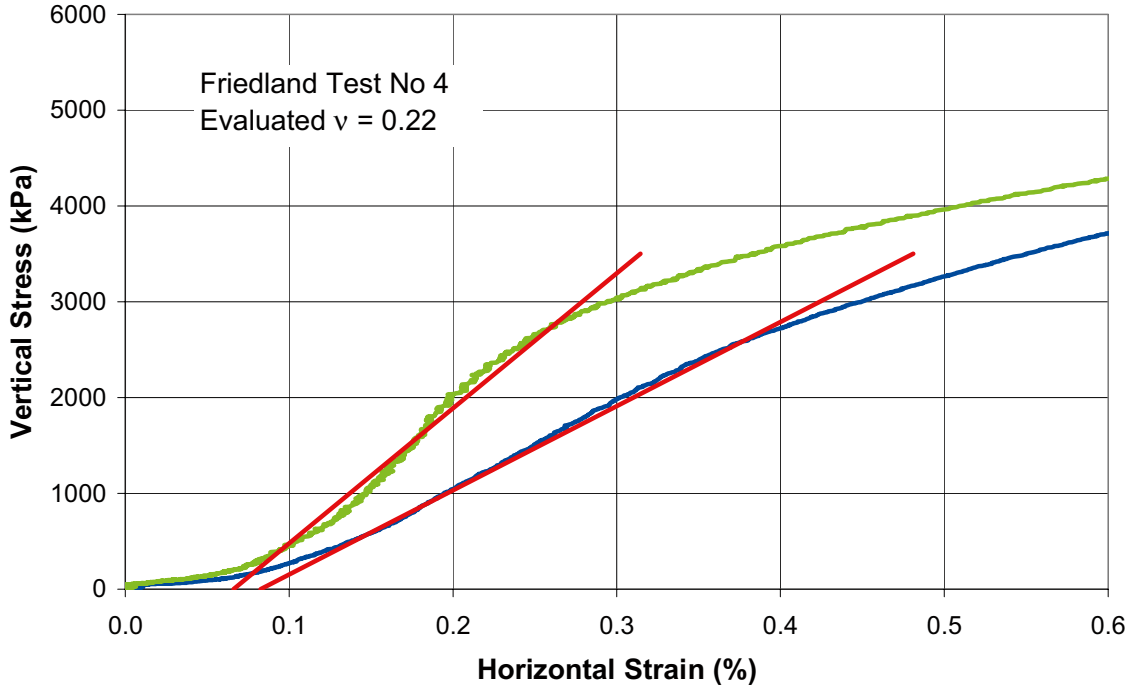
Friedland Test No 4
Evaluated ν = 0.22
Vertical Stress (kPa)
Horizontal Strain (%)
6000
5000
4000
3000
2000
1000
0
0.0
0.1
0.2
0.3
0.4
0.5
0.6

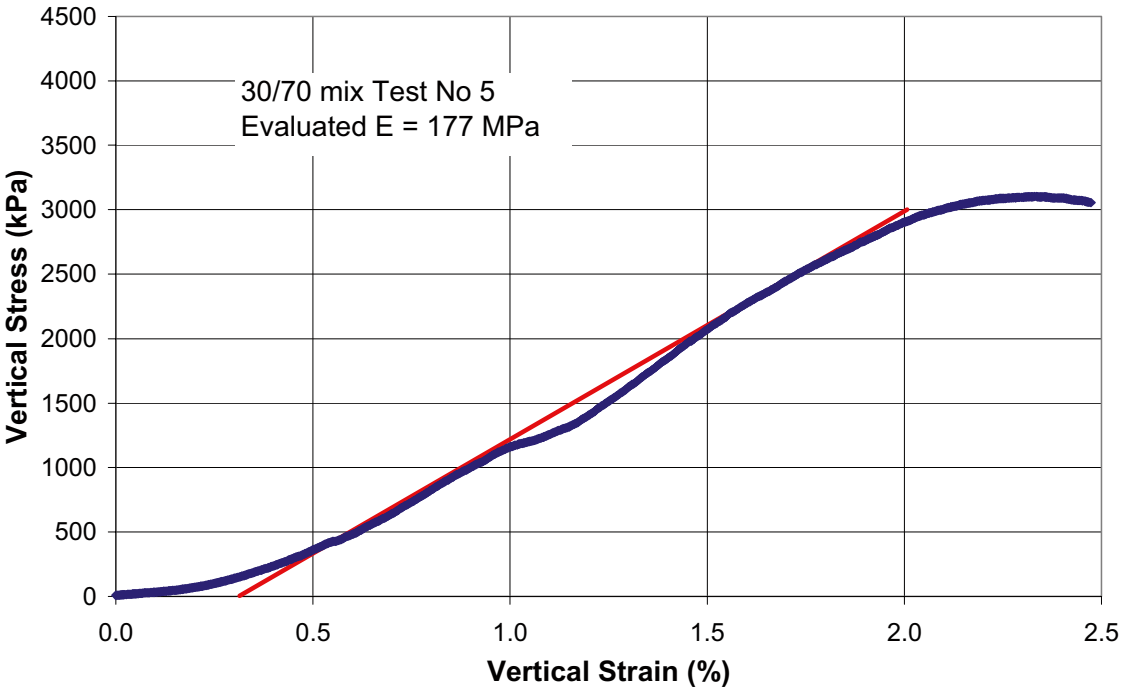
30/70 mix Test No 5
Evaluated E = 177 MPa
Vertical Stress (kPa)
4500
4000
3500
3000
2500
2000
1500
1000
500
0
0.0
0.5
1.0
1.5
2.0
2.5
Vertical Strain (%)

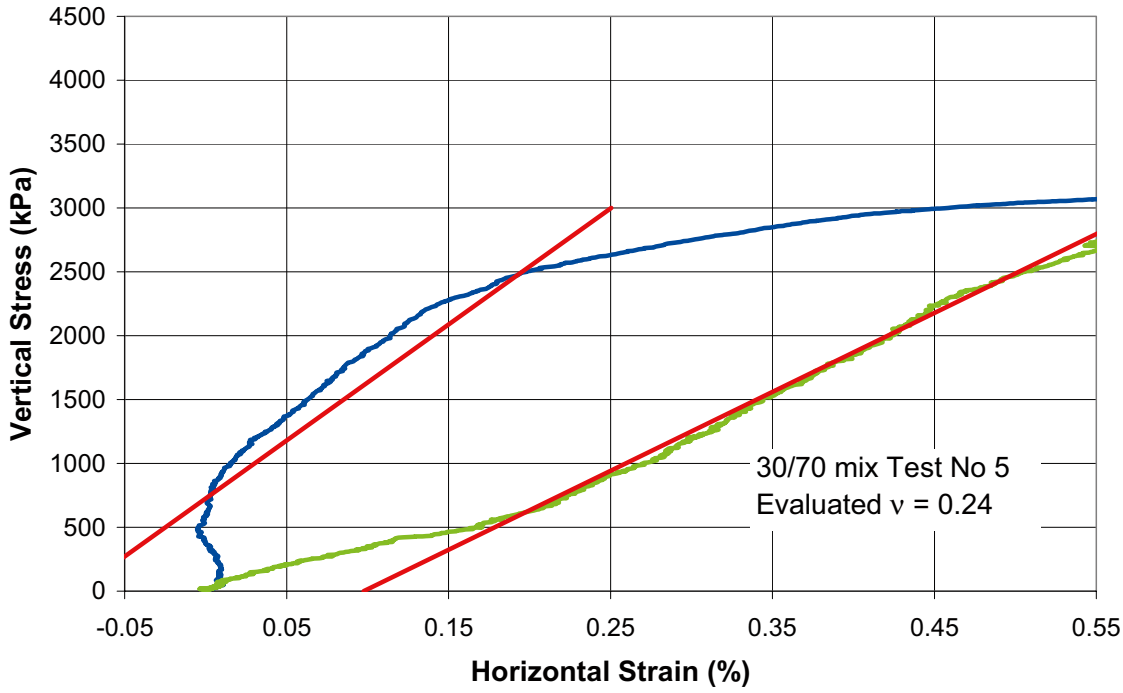
30/70 mix Test No 5
Evaluated ν = 0.24
Vertical Stress (kPa)
4500
4000
3500
3000
2500
2000
1500
1000
500
0
-0.05
0.05
0.15
0.25
0.35
0.45
0.55
Horizontal Strain (%)

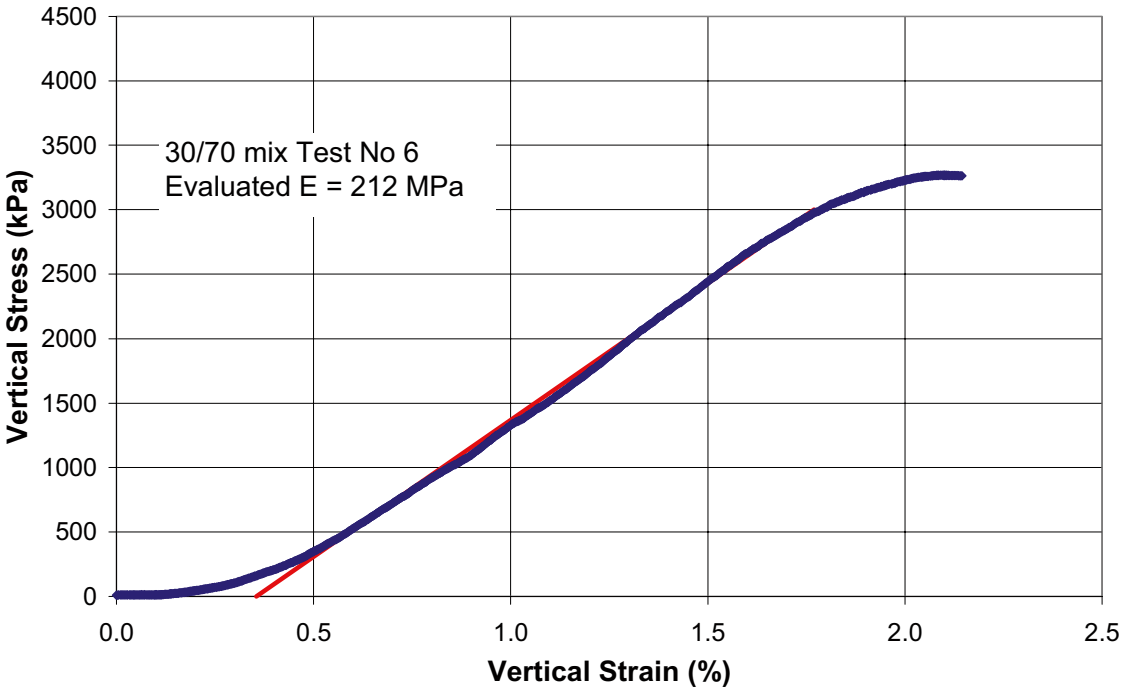
30/70 mix Test No 6
Evaluated E = 212 MPa
Vertical Stress (kPa)
4500
4000
3500
3000
2500
2000
1500
1000
500
0
0.0
0.5
1.0
1.5
2.0
2.5
Vertical Strain (%)

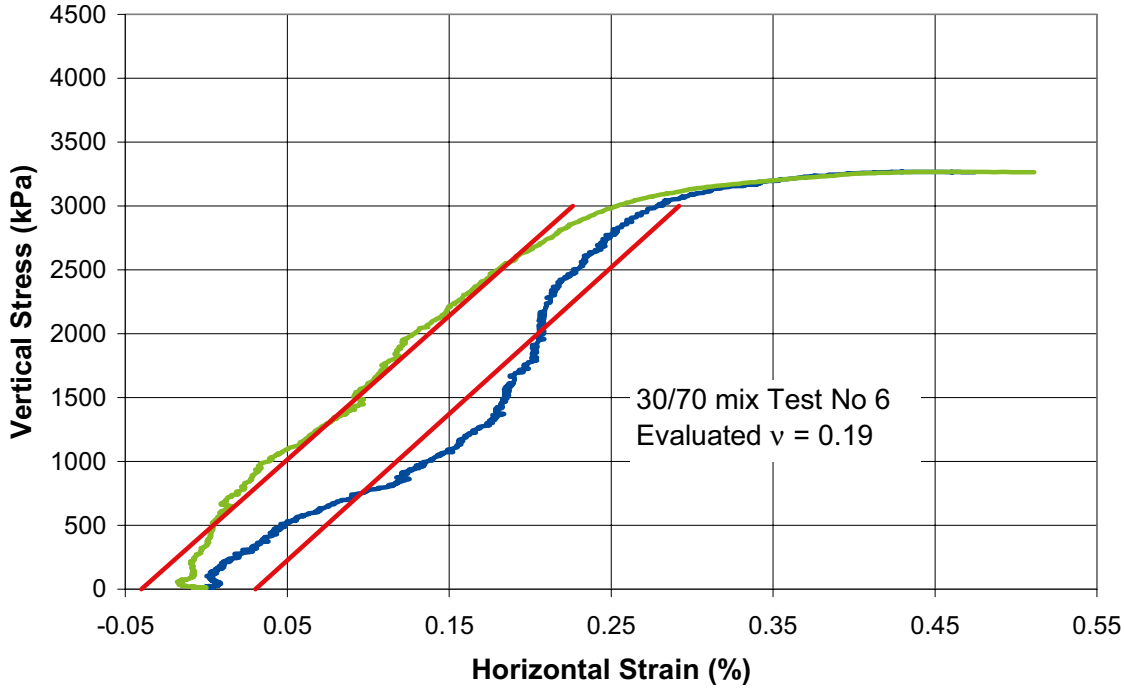
30/70 mix Test No 6
Evaluated ν = 0.19
Vertical Stress (kPa)
4500
4000
3500
3000
2500
2000
1500
1000
500
0
-0.05
0.05
0.15
0.25
0.35
0.45
0.55
Horizontal Strain (%)

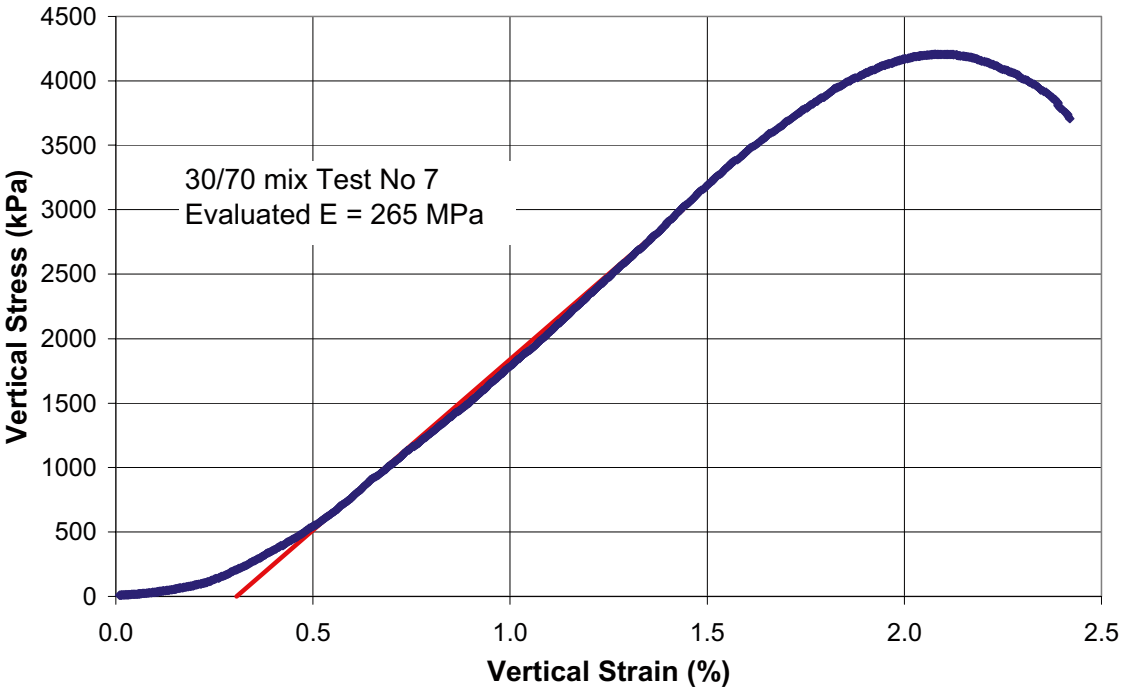
30/70 mix Test No 7
Evaluated E = 265 MPa
Vertical Stress (kPa)
Vertical Strain (%)
4500
4000
3500
3000
2500
2000
1500
1000
500
0
0.0
0.5
1.0
1.5
2.0
2.5

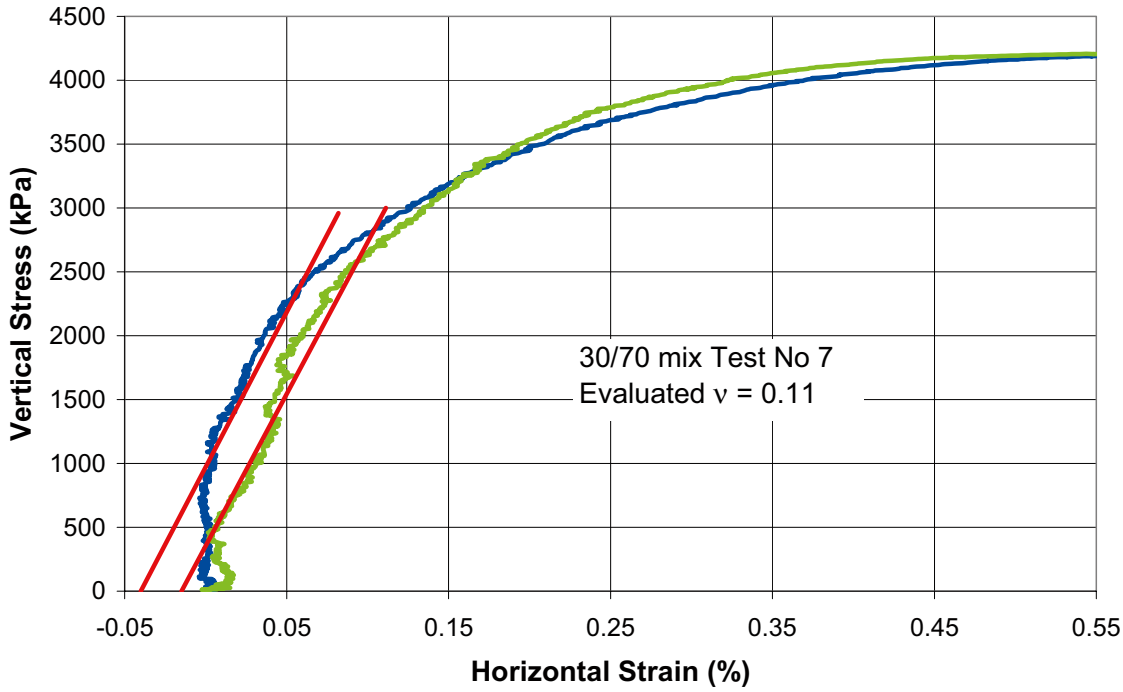
30/70 mix Test No 7
Evaluated ν = 0.11
Vertical Stress (kPa)
Horizontal Strain (%)
4500
4000
3500
3000
2500
2000
1500
1000
500
0
-0.05
0.05
0.15
0.25
0.35
0.45
0.55

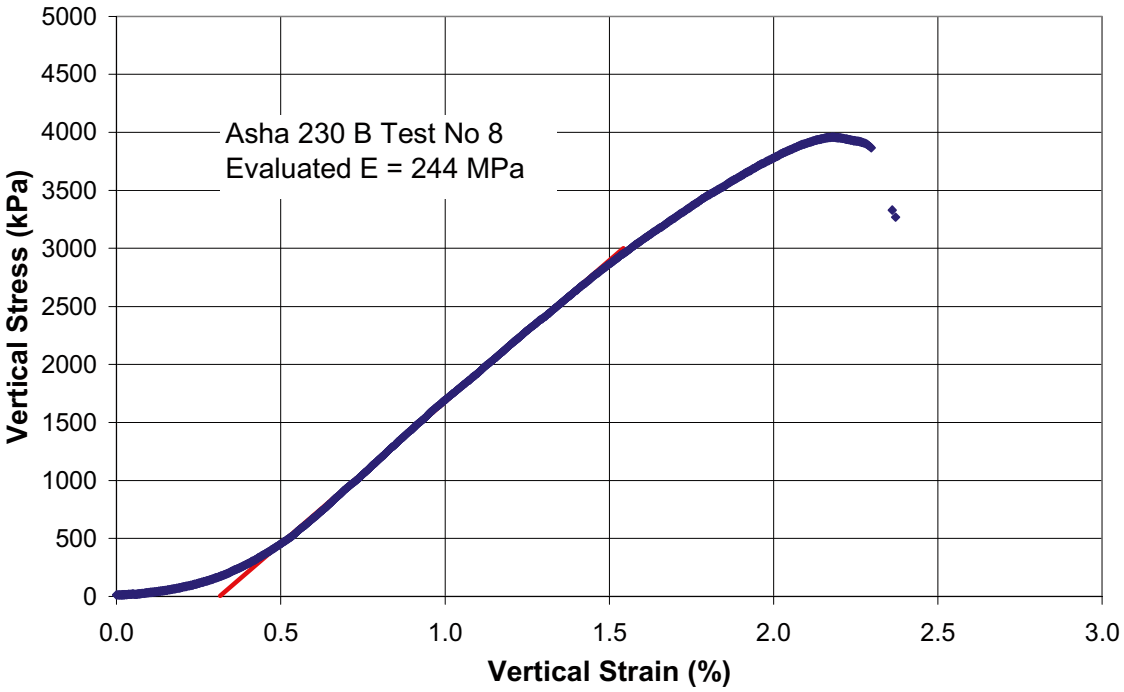
Asha 230 B Test No 8
Evaluated E = 244 MPa
Vertical Stress (kPa)
5000
4500
4000
3500
3000
2500
2000
1500
1000
500
0
0.0
0.5
1.0
1.5
2.0
2.5
3.0
Vertical Strain (%)

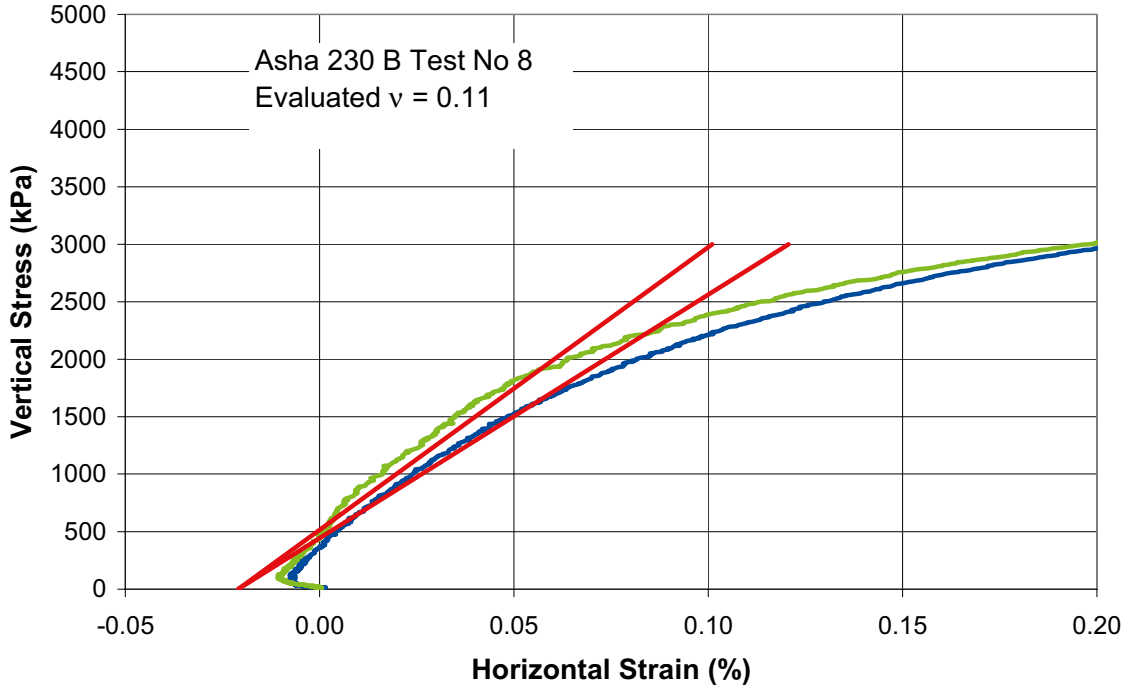
Asha 230 B Test No 8
Evaluated ν = 0.11
Vertical Stress (kPa)
5000
4500
4000
3500
3000
2500
2000
1500
1000
500
0
-0.05
0.00
0.05
0.10
0.15
0.20
Horizontal Strain (%)

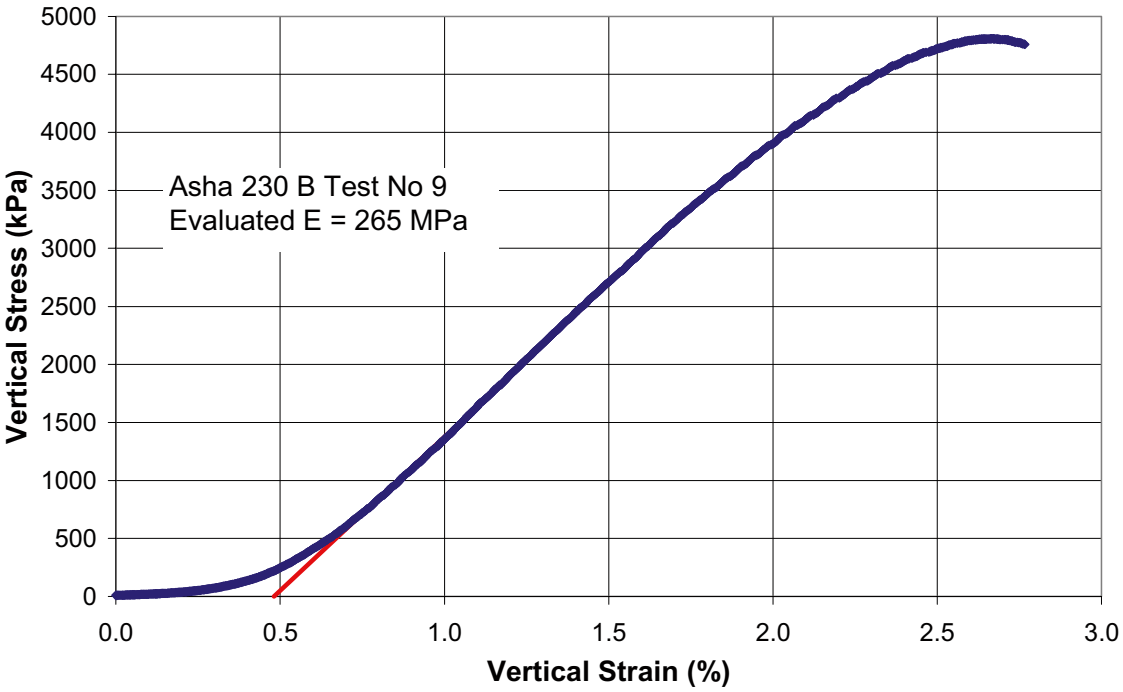
Asha 230 B Test No 9
Evaluated E = 265 MPa
Vertical Stress (kPa)
Vertical Strain (%)
5000
4500
4000
3500
3000
2500
2000
1500
1000
500
0
0.0
0.5
1.0
1.5
2.0
2.5
3.0

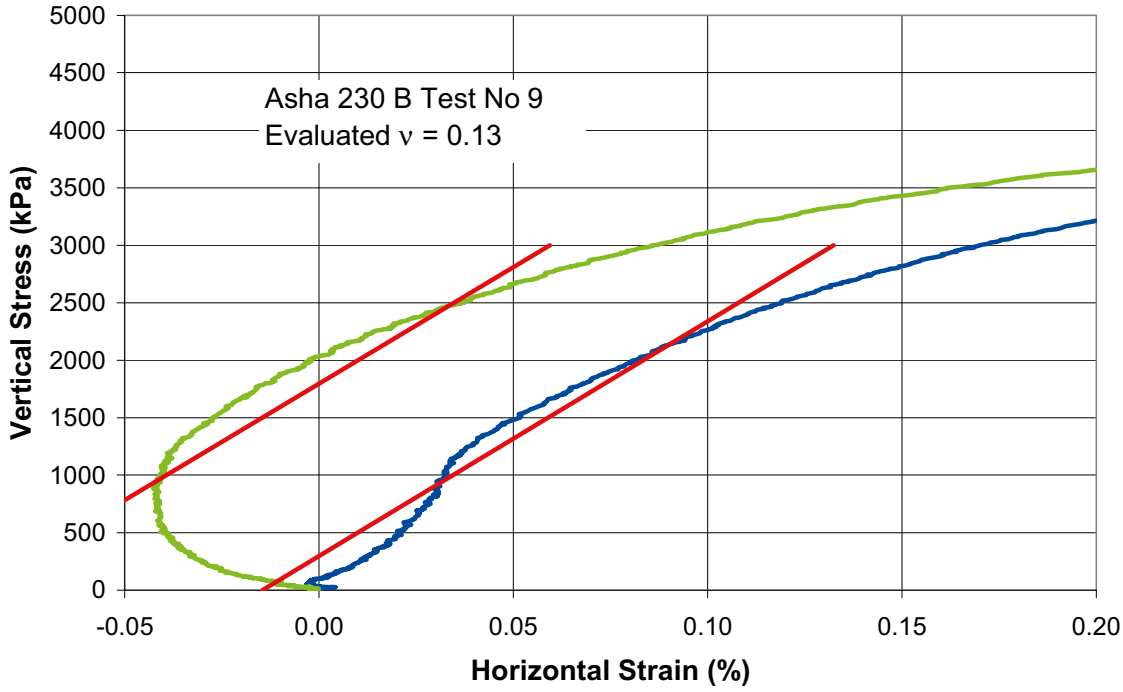
Asha 230 B Test No 9
Evaluated ν = 0.13
Vertical Stress (kPa)
Horizontal Strain (%)
5000
4500
4000
3500
3000
2500
2000
1500
1000
500
0
-0.05
0.00
0.05
0.10
0.15
0.20

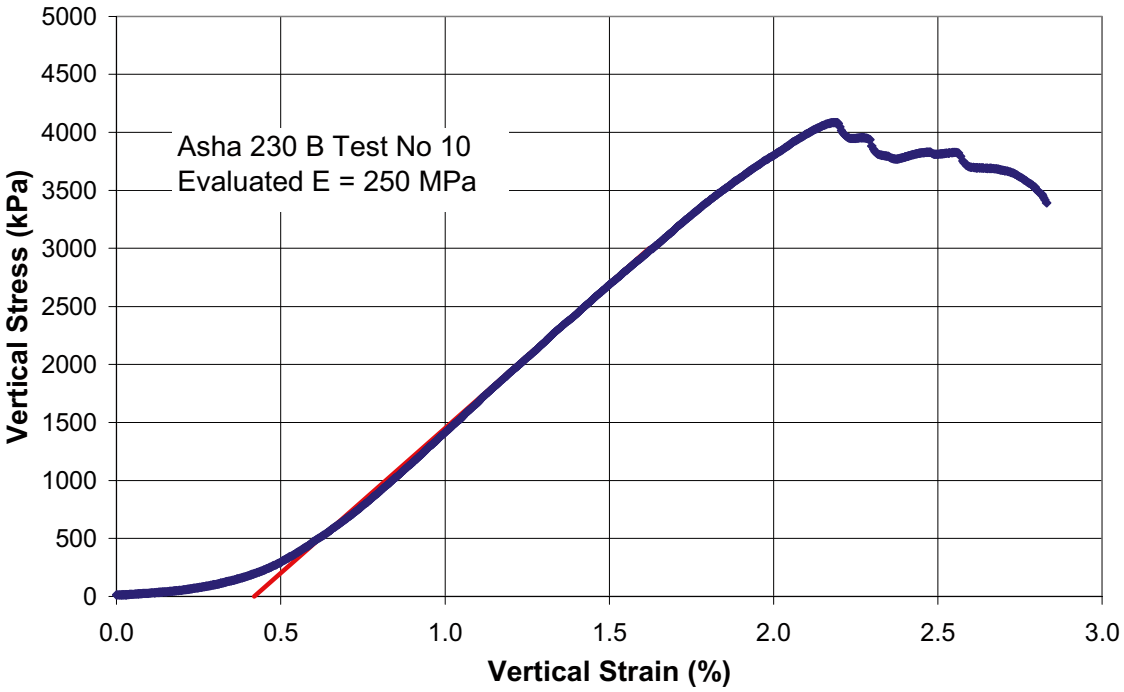
Asha 230 B Test No 10
Evaluated E = 250 MPa
Vertical Stress (kPa)
5000
4500
4000
3500
3000
2500
2000
1500
1000
500
0
0.0
0.5
1.0
1.5
2.0
2.5
3.0
Vertical Strain (%)

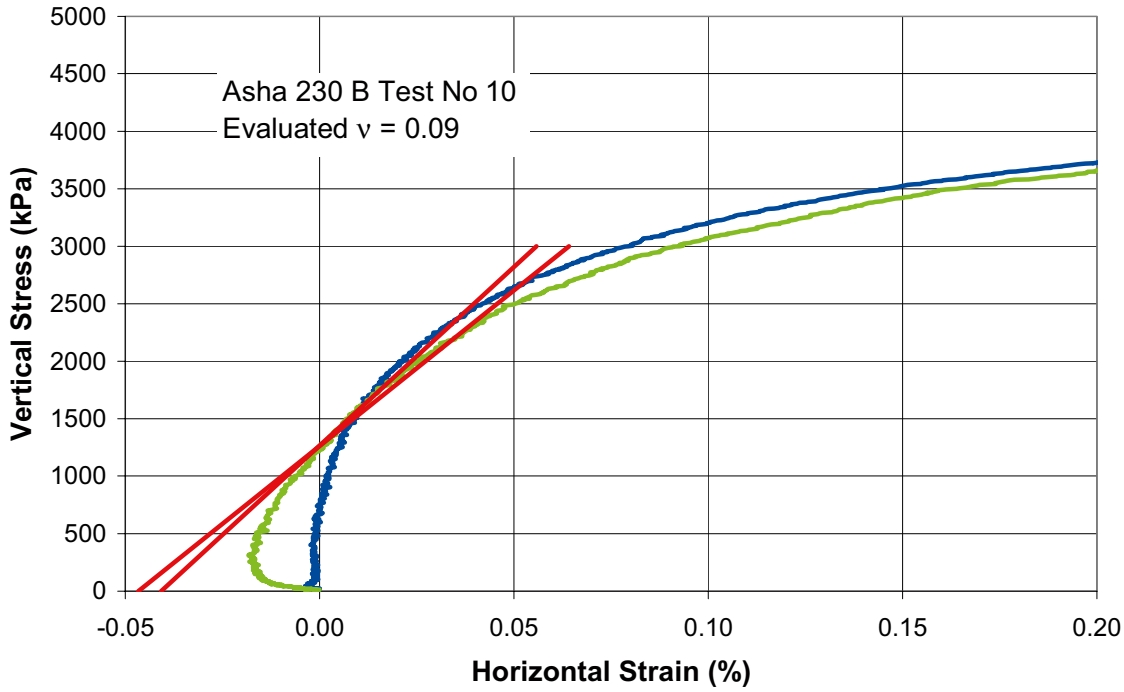
Asha 230 B Test No 10
Evaluated ν = 0.09
Vertical Stress (kPa)
5000
4500
4000
3500
3000
2500
2000
1500
1000
500
0
-0.05
0.00
0.05
0.10
0.15
0.20
Horizontal Strain (%)

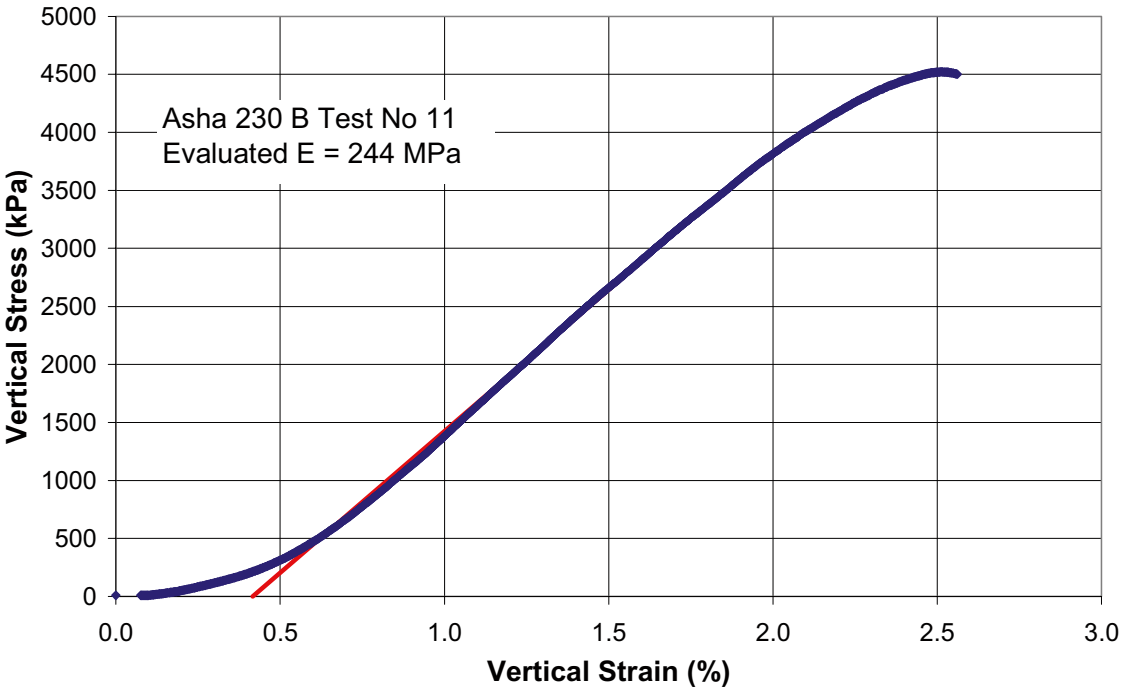
Asha 230 B Test No 11
Evaluated E = 244 MPa
Vertical Stress (kPa)
5000
4500
4000
3500
3000
2500
2000
1500
1000
500
0
0.0
0.5
1.0
1.5
2.0
2.5
3.0
Vertical Strain (%)

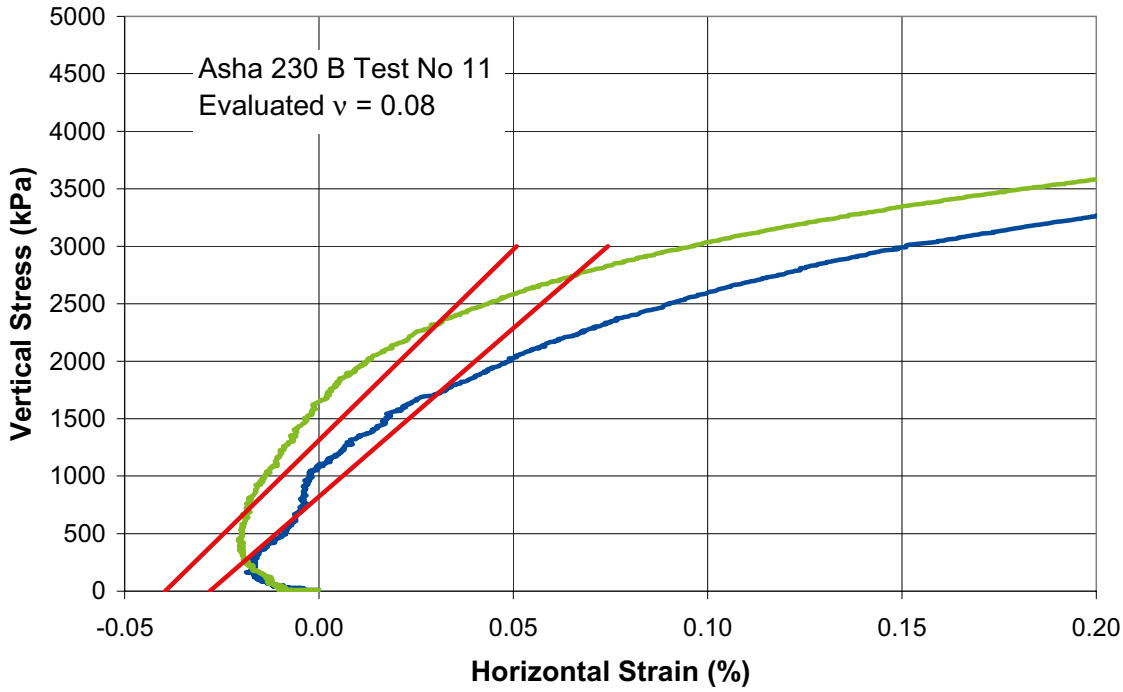
Asha 230 B Test No 11
Evaluated ν = 0.08
Vertical Stress (kPa)
5000
4500
4000
3500
3000
2500
2000
1500
1000
500
0
-0.05
0.00
0.05
0.10
0.15
0.20
Horizontal Strain (%)

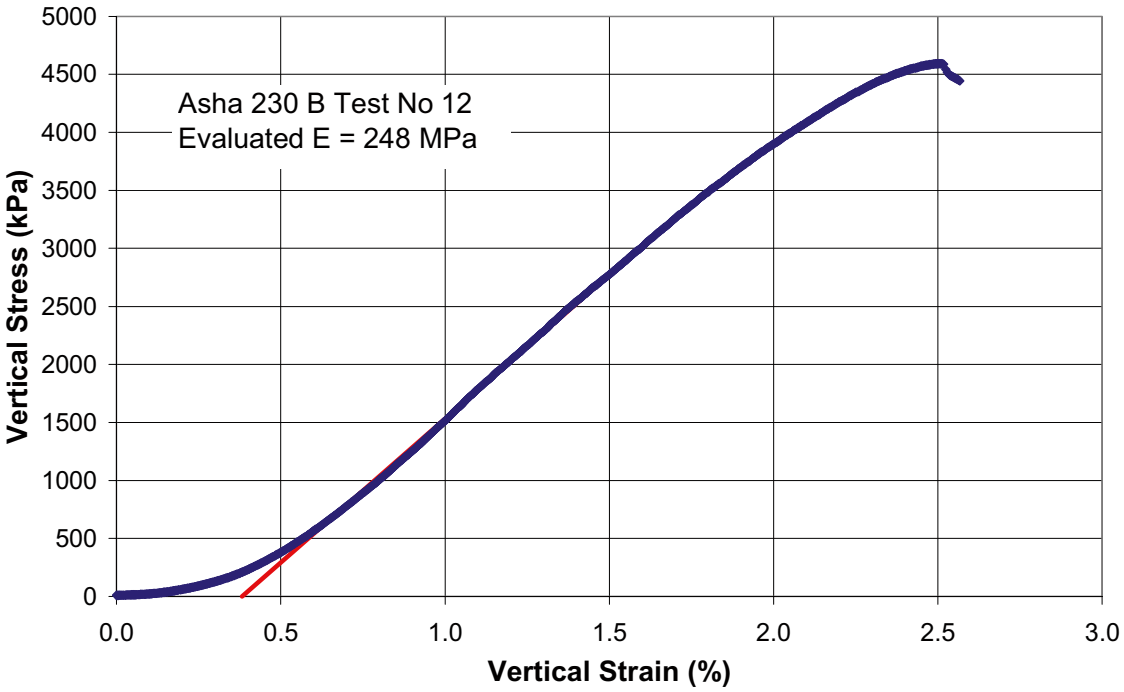
Asha 230 B Test No 12
Evaluated E = 248 MPa
Vertical Stress (kPa)
5000
4500
4000
3500
3000
2500
2000
1500
1000
500
0
0.0
0.5
1.0
1.5
2.0
2.5
3.0
Vertical Strain (%)

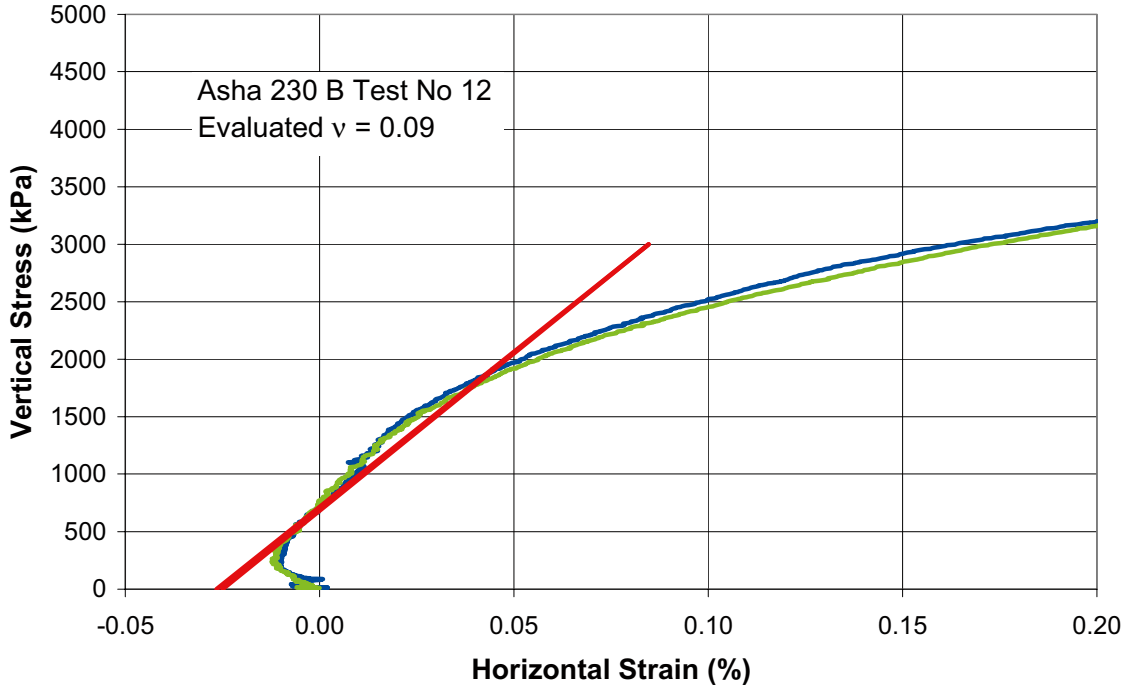
Asha 230 B Test No 12
Evaluated ν = 0.09
Vertical Stress (kPa)
5000
4500
4000
3500
3000
2500
2000
1500
1000
500
0
-0.05
0.00
0.05
0.10
0.15
0.20
Horizontal Strain (%)

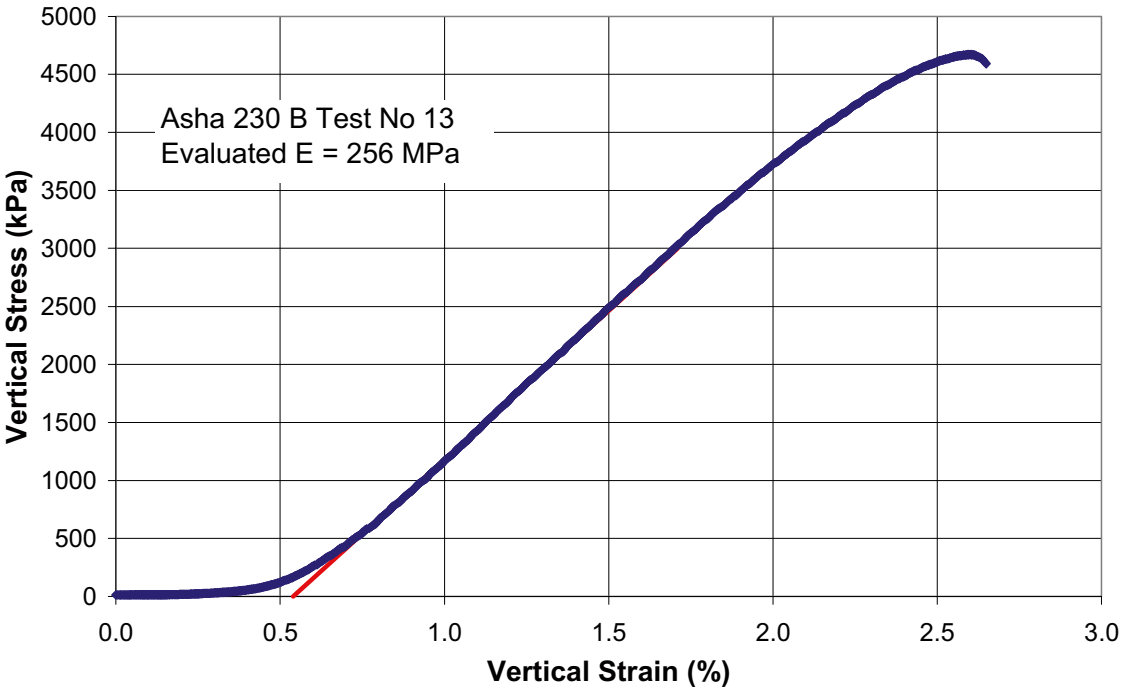
Asha 230 B Test No 13
Evaluated E = 256 MPa
Vertical Stress (kPa)
5000
4500
4000
3500
3000
2500
2000
1500
1000
500
0
0.0
0.5
1.0
1.5
2.0
2.5
3.0
Vertical Strain (%)

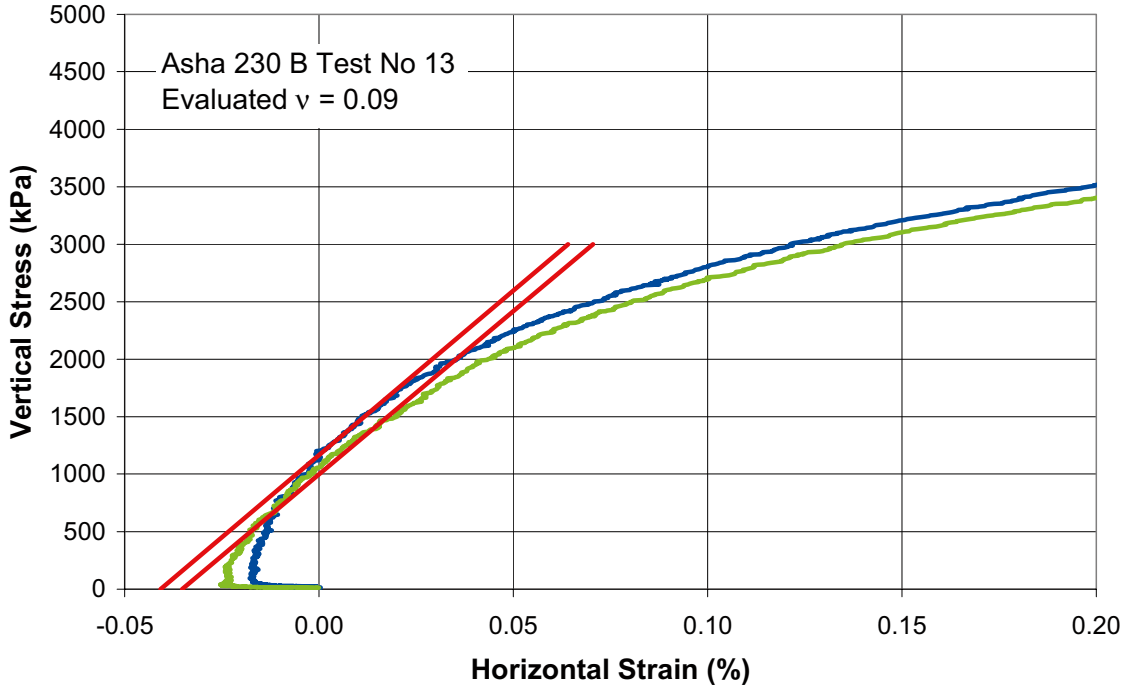
Asha 230 B Test No 13
Evaluated ν = 0.09
Vertical Stress (kPa)
5000
4500
4000
3500
3000
2500
2000
1500
1000
500
0
-0.05
0.00
0.05
0.10
0.15
0.20
Horizontal Strain (%)

Appendix 2

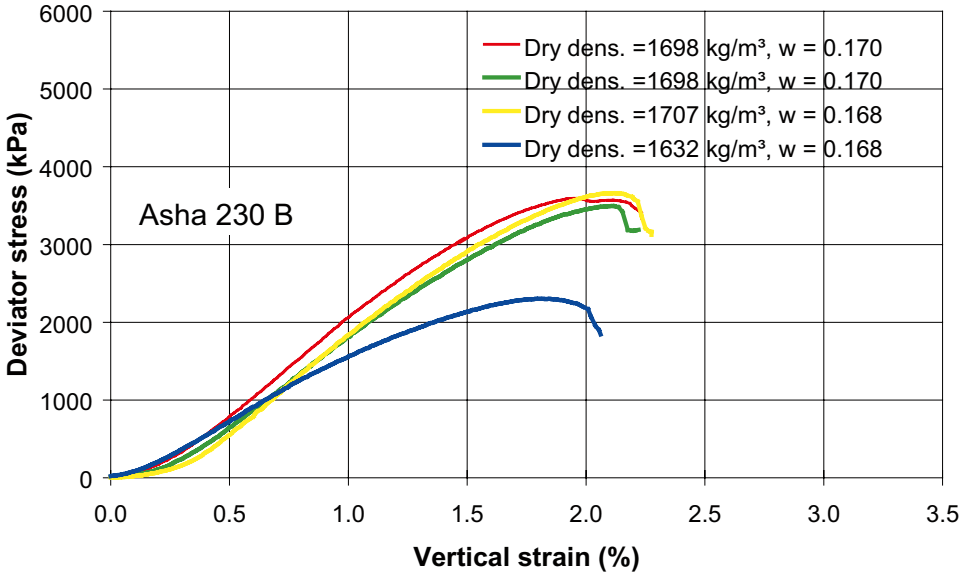
Asha 230 B
Dry dens. =1698 kg/m³, w = 0.170
Dry dens. =1698 kg/m³, w = 0.170
Dry dens. =1707 kg/m³, w = 0.168
Dry dens. =1632 kg/m³, w = 0.168
Deviator stress (kPa)
Vertical strain (%)

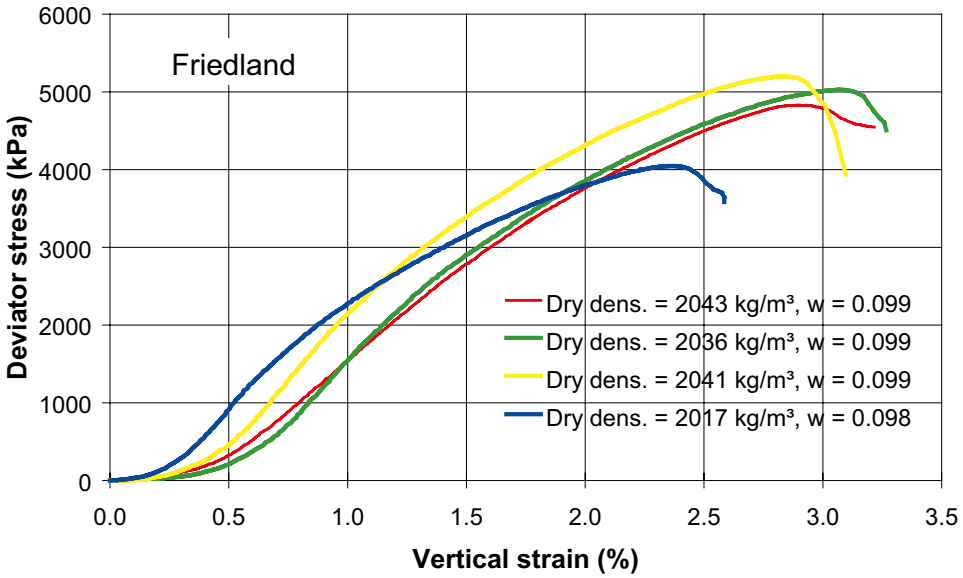
Friedland
Dry dens. = 2043 kg/m³, w = 0.099
Dry dens. = 2036 kg/m³, w = 0.099
Dry dens. = 2041 kg/m³, w = 0.099
Dry dens. = 2017 kg/m³, w = 0.098
Deviator stress (kPa)
Vertical strain (%)

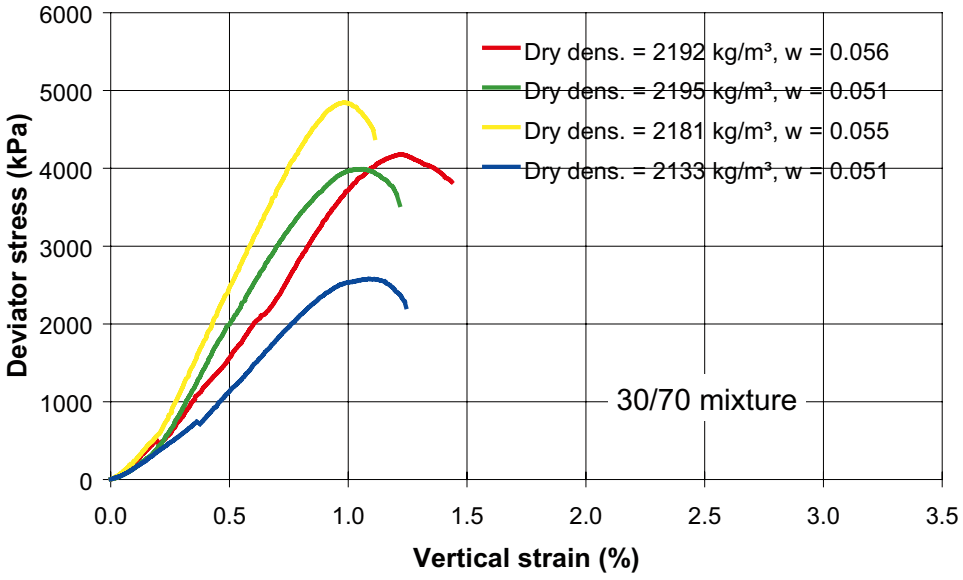
Dry dens. = 2192 kg/m³, w = 0.056
Dry dens. = 2195 kg/m³, w = 0.051
Dry dens. = 2181 kg/m³, w = 0.055
Dry dens. = 2133 kg/m³, w = 0.051
30/70 mixture
Deviator stress (kPa)
Vertical strain (%)

Appendix 3

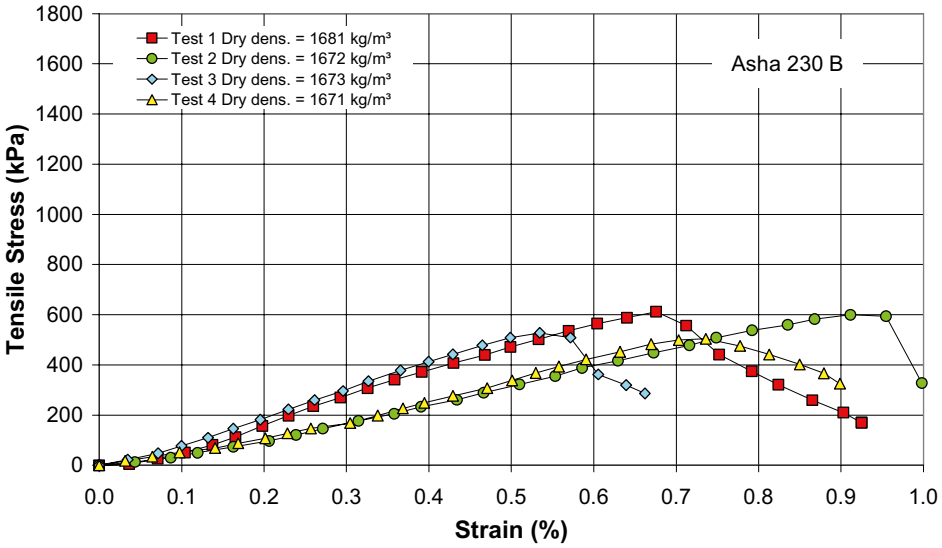
Test 1 Dry dens. = 1681 kg/m³
Test 2 Dry dens. = 1672 kg/m³
Test 3 Dry dens. = 1673 kg/m³
Test 4 Dry dens. = 1671 kg/m³
Asha 230 B
Tensile Stress (kPa)
Strain (%)

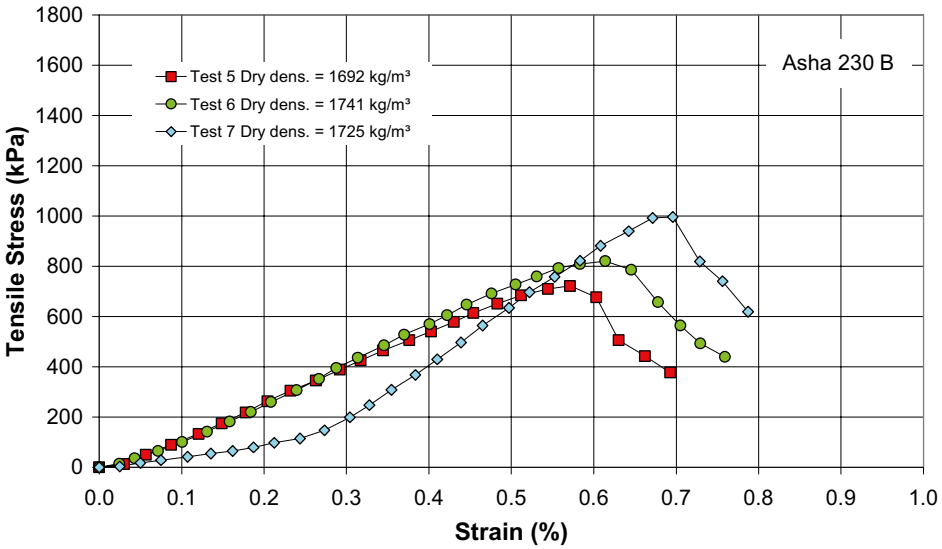
Test 5 Dry dens. = 1692 kg/m³
Test 6 Dry dens. = 1741 kg/m³
Test 7 Dry dens. = 1725 kg/m³
Asha 230 B
Tensile Stress (kPa)
Strain (%)

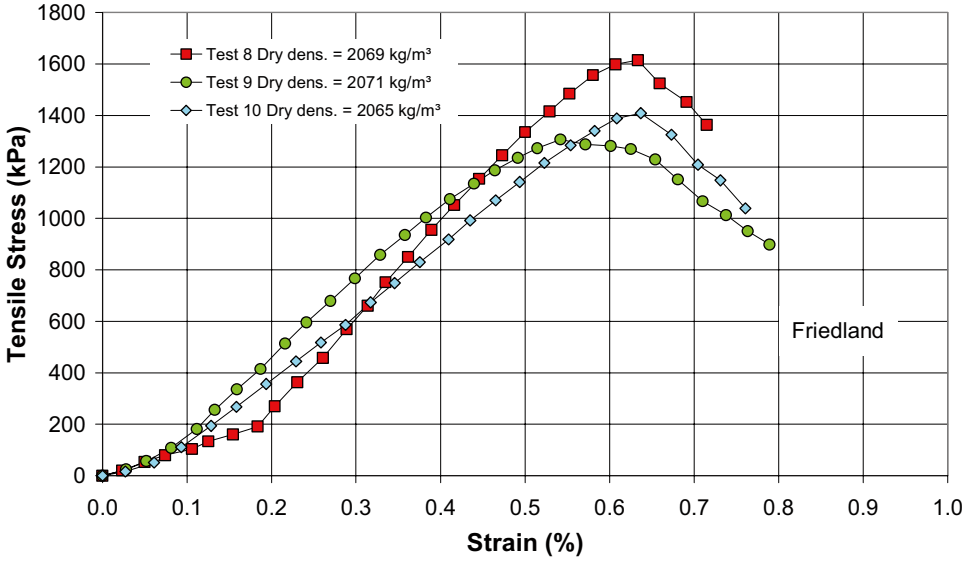
Test 8 Dry dens. = 2069 kg/m³
Test 9 Dry dens. = 2071 kg/m³
Test 10 Dry dens. = 2065 kg/m³
Friedland
Tensile Stress (kPa)
Strain (%)

Appendix 4

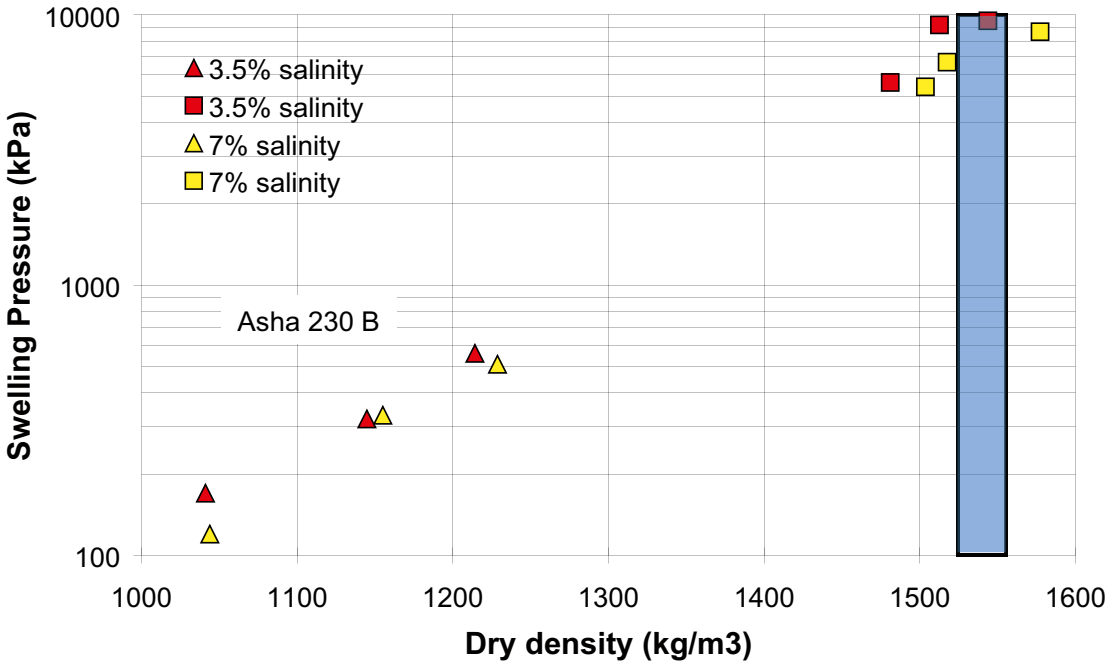
10000
1000
100
Swelling Pressure (kPa)
3.5% salinity
3.5% salinity
7% salinity
7% salinity
Asha 230 B
1000
1100
1200
1300
1400
1500
1600
Dry density (kg/m3)

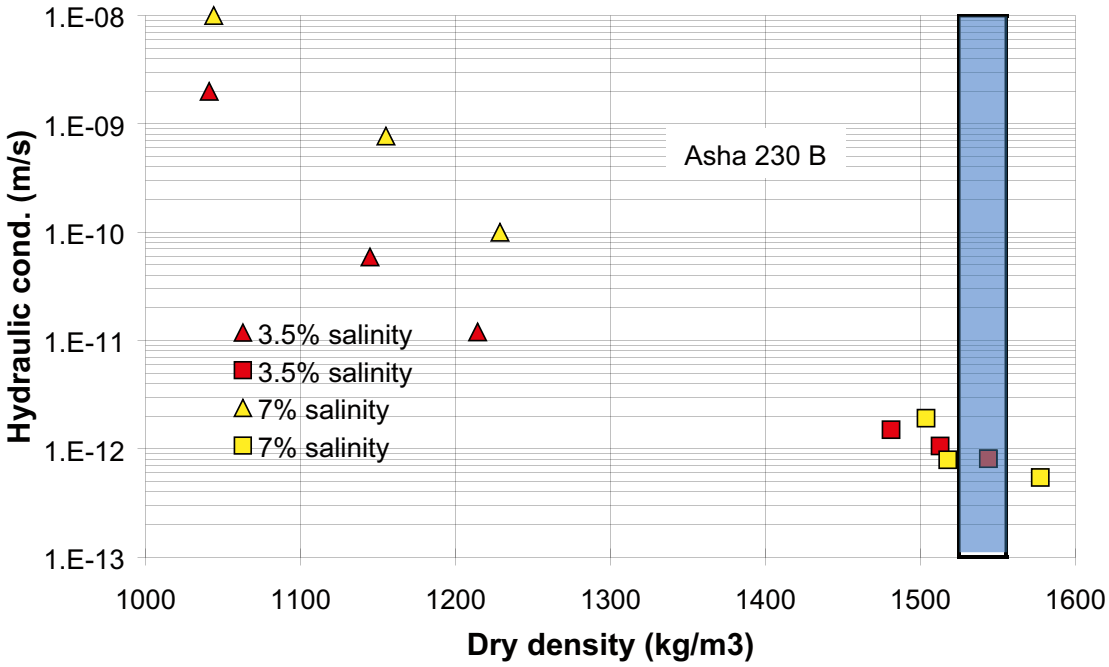
1.E-08
1.E-09
1.E-10
1.E-11
1.E-12
1.E-13
Hydraulic cond. (m/s)
Asha 230 B
3.5% salinity
3.5% salinity
7% salinity
7% salinity
1000
1100
1200
1300
1400
1500
1600
Dry density (kg/m3)

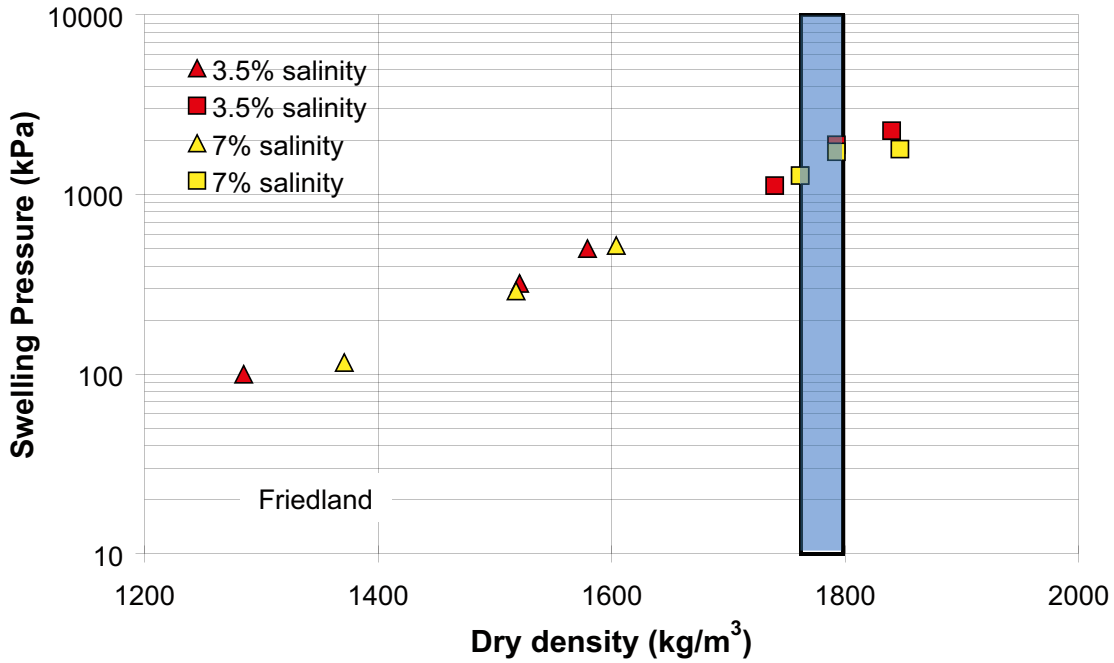
10000
1000
100
10
Swelling Pressure (kPa)
3.5% salinity
3.5% salinity
7% salinity
7% salinity
Friedland
1200
1400
1600
1800
2000
Dry density (kg/m3)

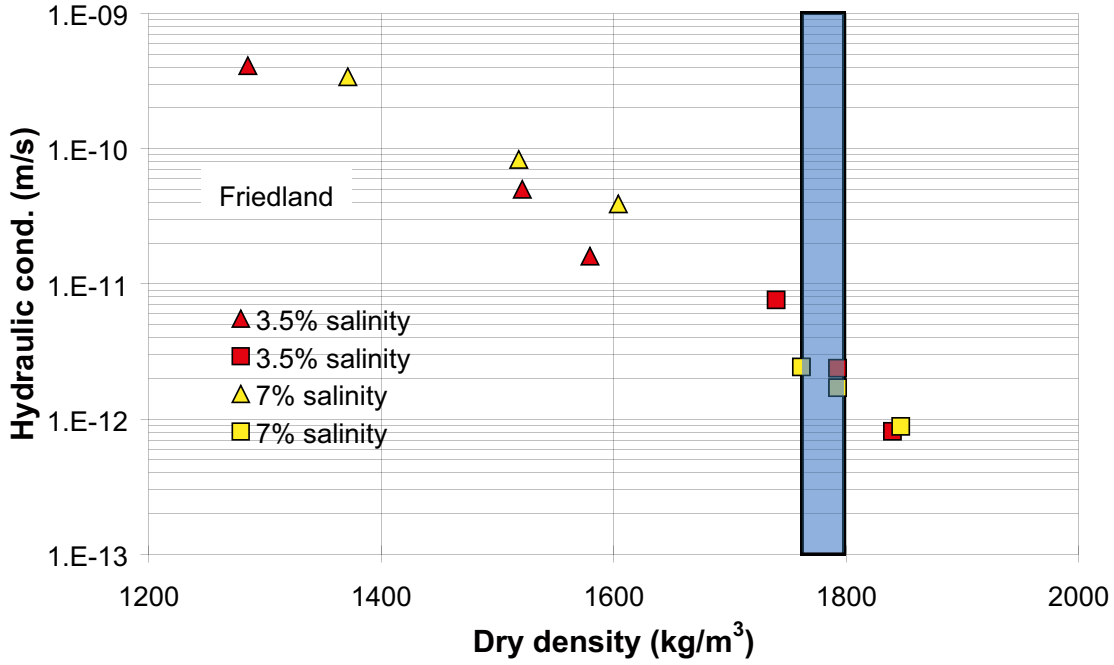
1.E-09
1.E-10
1.E-11
1.E-12
1.E-13
Hydraulic cond. (m/s)
Friedland
3.5% salinity
3.5% salinity
7% salinity
7% salinity
1200
1400
1600
1800
2000
Dry density (kg/m3)

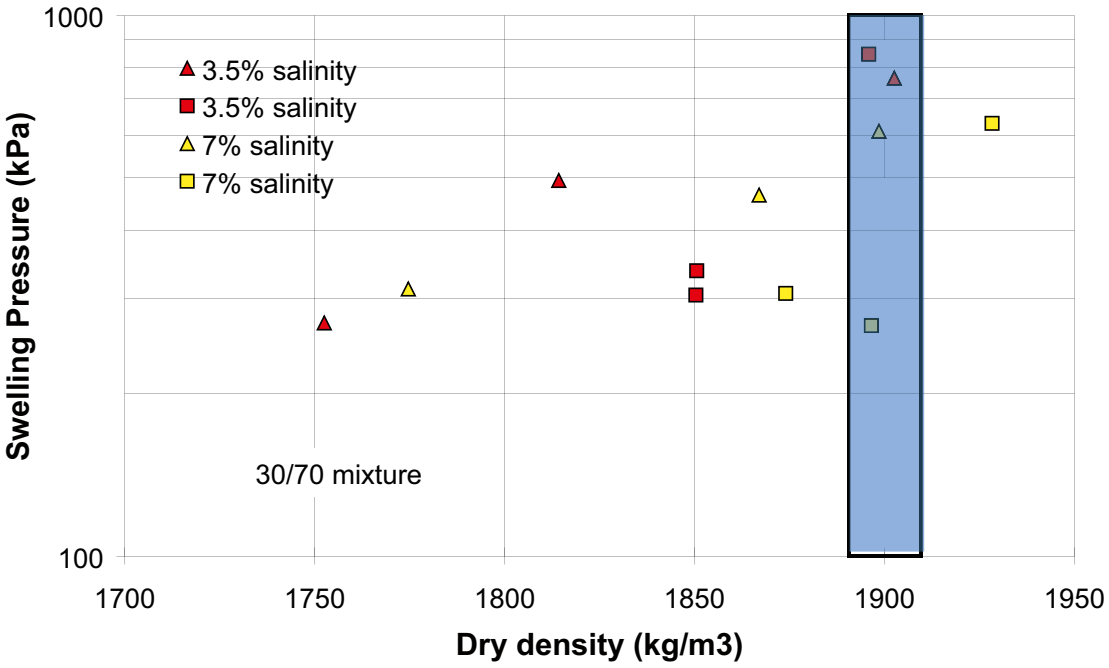
1000
100
Swelling Pressure (kPa)
3.5% salinity
3.5% salinity
7% salinity
7% salinity
30/70 mixture
1700
1750
1800
1850
1900
1950
Dry density (kg/m3)

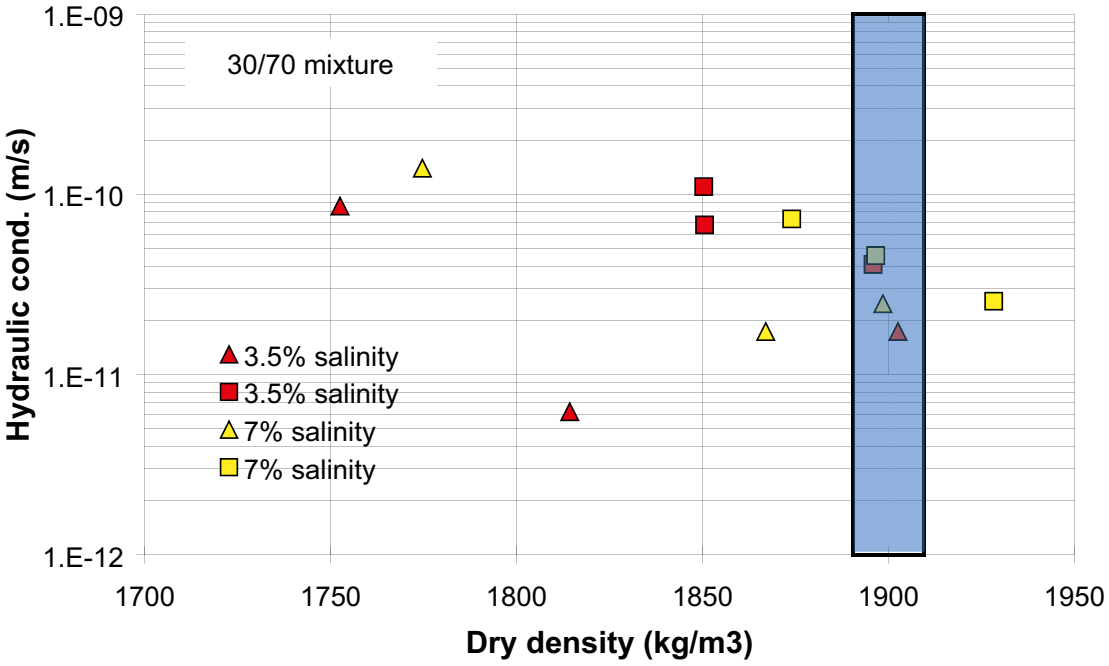
1.E-09
1.E-10
1.E-11
1.E-12
Hydraulic cond. (m/s)
30/70 mixture
3.5% salinity
3.5% salinity
7% salinity
7% salinity
1700
1750
1800
1850
1900
1950
Dry density (kg/m3)

Appendix 5

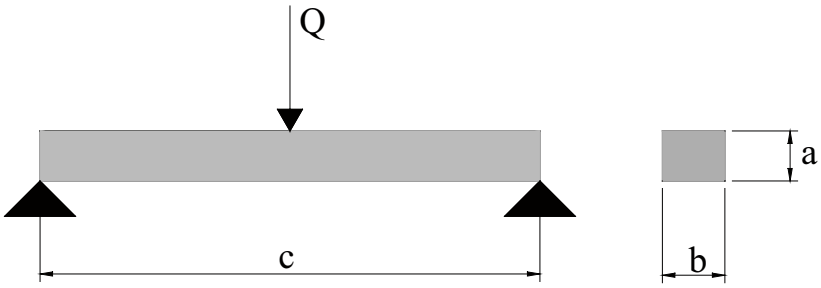

The area moment of inertia for the beam shown in the picture above can be expressed as

$$I = \frac{ba^3}{12} \tag{1}$$

The maximum moment (M_{max}) for the beam can be calculated as

$$M_{\max} = \frac{Qc}{4} \tag{2}$$

Corresponding maximum vertical displacement (ω) can be expressed as

$$\omega = \frac{Qc^3}{48EI} \tag{3}$$

where
E = Young's modulus

From equation 3 the Young's modulus can be evaluated as

$$E = \frac{Qc^3}{48I\omega} \tag{4}$$

The maximum tensile stress for the beam can be expressed as

$$\sigma_t = \frac{M_{\max} a}{2I} \tag{5}$$

Combining equations 1, 2 and 5 the maximum tensile stress can be expressed as

$$\sigma_t = \frac{6Qc}{4ba^2} \tag{6}$$

According to Hook's law the maximum tensile strain for the beam can be expressed as

$$\varepsilon_t = \frac{\sigma_t}{E} \tag{7}$$

Combining equations 1, 4, 6 and 7 the maximum tensile stress can be expressed as

$$\varepsilon_t = \frac{a\omega 6}{c^2} \tag{8}$$

Appendix 6

The stress around a weightless slice of the saturated bentonite in a deposition hole is shown in the figure below

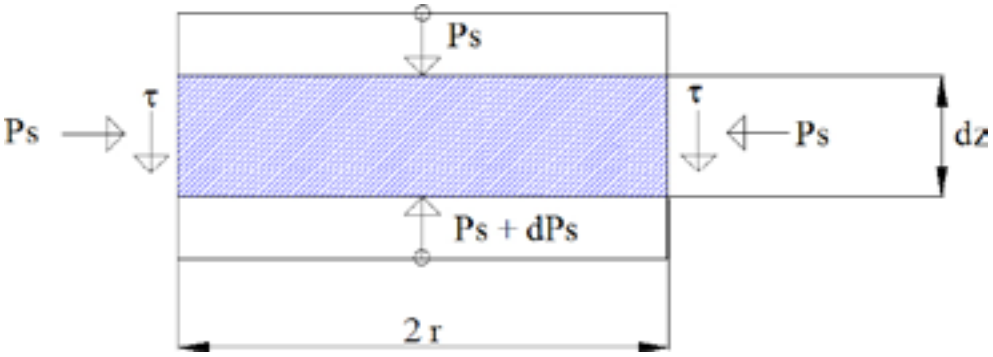

where
p_s = swelling pressure
τ = shear stress between the bentonite and the rock ($\tau = p_s \times \tan(\phi)$)
r = radius of the deposition hole

The force balance for the element is as follows:

$$dp_s \times \pi \times r^2 = p_s \times \tan(\phi) \times 2 \times \pi \times r \times dz$$

$$\frac{dp_s}{p_s} = \tan(\phi) \times \frac{2}{r} \times d_z$$

$$d_z = \frac{r}{2x \tan(\phi)} \times \frac{dp_s}{p_s}$$

$$\int_0^z dz = \frac{r}{2 \times \tan(\phi)} \int_{p_{sb}}^{p_{sa}} \frac{dp_s}{p_s}$$

$$z = \frac{r}{2 \times \tan(\phi)} (\ln p_{sa} - \ln p_{sb})$$

$$P_{sa} = P_{sb} \times e^{-\left(\frac{2z \tan(\phi)}{r}\right)}$$